NTNU – Trondheim
Norwegian University of
Science and Technology

Radio Tracking of Open Range Sheep

Methods for Radio Location in a Sub-GHz
Base Station Network

Snorre Haugstulen Olsen

Problem Description

Candidate name: Snorre Haugstulen Olsen

Thesis title: Radio Tracking of Open Range Sheep: Methods for Radio Location in a Sub-GHz Base Station Network

Problem Description: Every year in Norway, a total of 2 000 000 sheep are released in unfenced mountain/forest ranges for summer grazing. Approximately 120 000 perish every season, out of which a high percentage is lambs. These numbers are declared unacceptable by the Norwegian Ministry of Agriculture and Food, and research is directed into cutting these losses. At NTNU a cooperation project between the Institute of Computer Science and the Institute of Electronics and Telecommunications aims to develop a radio tracking and communication system to inform the farmers about their sheep's whereabouts as well as other information such as physiological data.

This project investigates the possibility of locating sheep *without* using GPS technology on each individual, due to the high energy demands of GPS receivers. The system will use a Texas Instruments chip in the CC112x series, operating in the sub-GHz band. What methods of location may be employed in the system, given multiple base stations at known, fixed locations? With what accuracy can sheep be located and tracked?

Supervisor: Morten Olavsbråten

Abstract

This thesis aims to compare methods of radio location for the purpose of tracking sheep by using sub-GHz radio transceivers arranged in a base station network. Nearly 10% of free-grazing sheep in Norway are lost every year, creating losses for both farmers and the government. Tracking technology may reduce these losses.

Existing tracking solutions based on GPS and GSM are commercially available, but previous research shows that poor signal conditions in grazing areas limit their efficacy. An alternative tracking system using the low-power CC1120 transceiver from Texas Instruments is outlined and evaluated for the two following methods of radio location. *Hyperbolic trilateration* uses time difference of arrival (TDoA) estimates for receiver pairs and *circular trilateration* uses received signal strength (RSSI) to perform radio location.

Initial measurements show that the transceiver alone should not be used for TDoA estimation because its trigger signals are only accurate to within 25% of the predetermined symbol interval. In future work, TDoA can be estimated by comparing the bit streams taken directly from the A/D-converter (ADC) of two base stations. This requires additional hardware but is expected to be accurate enough to locate sheep.

A small-scale outdoors radio location experiment was carried out using RSSI measurements from the CC1120, and circular trilateration with three base stations approximately 200 m apart. A propagation model was fitted to calibration data using linear regression. Position estimates were calculated by both linear and non-linear least squares approximation using Matlab. The average error of the position estimates was 55.8 m. The error in the full-scale system for this method is estimated to be several kilometres, too large for tracking sheep.

In conclusion, the TDoA-based hyperbolic trilateration method is the only one showing promise. Challenges related to synchronicity between the base stations are expected to be met using GPS receivers. Additional work with extracting the bit streams is required before the TDoA can be estimated with sufficient accuracy.

Sammendrag

Oppgaven sammenligner fremgangsmåter for radiolokalisering ved bruk av sub-GHz radiomottakere i et basestasjonsnettverk. Rundt 10% av sauer på utmarksbeite i Norge går tapt hvert år, noe som skaper kostnader for både bønder og staten. Sporingsteknologi kan bidra til å redusere disse tapene.

Eksisterende sporingsløsninger basert på GPS og GSM er tilgjengelige, men tidligere forskning viser at dårlige signalforhold i beiteområdene begrenser effektiviteten til disse. Et alternativt system for sporing ved hjelp av lav-effekt transceiveren CC1120 fra Texas Instruments er skissert og vurdert mot de to følgende metoder for radiolokalisering. *Hyperbolsk trilaterering* bruker den estimerte tidsforskjellen i mottak (TDoA) for basestasjonpar og *sirkulær trilaterering* bruker den mottatte signalstyrken (RSSI) for å utføre radiolokalisering.

Innledende målinger viser at transceiveren alene ikke bør brukes for TDoA-estimering fordi trigger-signalene som kan brukes bare er nøyaktige inntil 25% av det forhåndsbestemte symbolintervallet. I fremtidig arbeid kan TDoA-estimeringen gjøres ved å sammenligne bit-strømmer hentet direkte fra A / D-omformeren (ADC) til to basestasjoner. Dette krever ekstra maskinvare, men er forventet nøyaktig nok til å finne sauene.

Et eksperiment for utendørs radiolokalisering i liten skala ble utført ved å benytte RSSI-målinger fra CC1120, og sirkulær trilaterering med tre basestasjoner ca 200 m fra hverandre. Propagasjonsmodellen ble tilpasset kalibreringsdata ved hjelp av lineær regresjon. Posisjonene ble beregnet ved hjelp av både lineære og ikke-lineære minste kvadratfeil algoritmer ved hjelp av Matlab. Den gjennomsnittlige feilen i posisjonsestimatene var 55.8 m. Feilen i et fullskala system for denne metoden er anslått til å være flere kilometer, alt for stor for sporing sau.

Oppsummeringsvis er den TDOA-baserte metoden for hyperbolsk trilaterering den eneste som viser lovende resultater. Utfordringer knyttet til synkronisitet mellom basestasjonene er forventet å kunne løses ved hjelp av GPS-mottakere. Videre arbeid med å hente ut bit-strømmene er nødvendig før TDoA-estimatene kan få tilstrekkelig nøyaktighet.

Preface

Writing this thesis has been interesting, challenging and at times frustrating; it started out with a very broad problem description and could have taken many different directions. A lot of time was put into learning how to program the transceiver before the thesis work could even begin. I have a few people I would like to thank for helping me get past the many obstacles that arose and gaining a lot of new knowledge on the way.

First of all, I have to thank my supervisor Morten Olavsbråten for somewhat narrowing down the problem, and providing guidance whenever my work strayed too far from what was realistically achievable.

Second, I am very grateful to Marius Ubostad and Trond Meckelborg Rognerud at Texas Instruments, Oslo for sharing hands-on experience and technical insight concerning the CC1120 transceiver that has been used in this thesis work.

Finally: thank you my dear Monika Anna Buganska for proofreading, invaluable support throughout the entire process and for playing the role of the sheep brilliantly in the trilateration experiment.

Contents

D Key Characteristics of the CC1120 **83**

Bibliography **85**

List of Figures

List of Tables

Abbreviations

ADC	**A**nalog to **Digital** **C**onverter
CRLB	**C**ramér **R**ao **L**ower **B**ound
DoA	**D**irection **of** **A**Arival
FPGA	**F**ield-**P**rogrammable **G**ate **A**rray
GPS	**G**lobal **P**osition **S**ystem
GPSDO	**GPS-Disciplined Oscillator**
IF	**I**ntermediate **Frequency**
ksps	**k**ilo **s**amples **p**er **s**econd
LSB	**L**east **Significant** **B**it
LoS	**L**ine **of** **S**ight
LVDS	**L**ow-**V**oltage **D**ifferential **S**ignalling
MSB	**M**ost **S**ignificant **B**it
OLS	**O**rdinare **L**east **Squares**
OCXO	**O**ven-**C**ontrolled **C**rystal **O**scillator
PLL	**P**hase **L**ocked **L**oop
RF	**R**adio (carrier) **F**requency
RMS	**R**oot **M**ean **S**quare
RSSI	**R**eceived **S**ignal **S**trength **I**ndicator
RoI	**R**egion **of** **I**nterest
TDMA	**T**ime **D**ivision **M**ultiple **A**ccess
TDoA	**T**ime **D**ifference **of** **A**rrival
ToA	**T**ime **of** **A**rrival
ToF	**T**ime **of** **F**light

Chapter 1

Introduction

1.1 Background and existing technology

This thesis is submitted as a partial fulfilment of a Master of Science degree in Electronics System Design and Innovation at the Norwegian University of Science and Technology. The thesis is written for the Department of Electronics and Telecommunication, as part of a collaboration with the Department of Computer Science and Information Technology to investigate the possibility of tracking sheep using cheap, energy efficient radio transceivers.

Within the guidelines specified in the problem text, various methods for positioning will be selected, examined and prototyped. The achievable accuracy will be highly dependent on tolerances in the hardware that is used. The goal of this project is to offer a viable alternative to existing GPS solutions. This means that the hardware cannot be too expensive, as the system will use dedicated base stations to locate the sheep.

This chapter details the motivation for tracking sheep grazing on the open range, and then moves on to a brief description of a few existing systems before specifying the guidelines provided for this thesis work.

1.1.1 Background

In the year 2012 about 1 900 000 sheep were released for free range grazing in Norway. Out of the 1.5 million animals grazing in registered coalitions 109 000 perished, a

loss of more than 7%. In $47\,000$ cases, applications were filed with the respective County Governor Offices for compensation for livestock presumably killed by one of Norway's five protected species of large predators: lynx, wolf, wolverine, bear and eagle. According to the Norwegian Environment Agency, farmers were paid a total of NOK 61 million in compensation for the $26\,500$ cases that were approved.[1]

Evidence that preserved predators were actually involved was presented in less than 10% of the cases where compensation was paid out. Common proof is the sheep's cadaver or fur/droppings from the predator. Without this kind of evidence the decision is based on the County Governor's best assessment, taking into account predator spotting in the area and nearby attacks.[1]

A system for electronic tracking of sheep may aid farmers not only in recovering cadavers early enough that they may serve as evidence, but also in recovering sheep that have gotten lost before they die. These latter cases may be animals that are physically stuck, or immobilized due to sickness. This means there is a double benefit to implement tracking:

- Lost animals may be found and saved before they die, cutting losses in livestock for farmers, and preventing such cases being interpreted as predator attacks based on circumstantial evidence. This cuts losses for the Norwegian Environment Agency as well as the farmers.

- Cadavers may be recovered early enough to prove attacks by protected predators, ensuring compensation for farmers.

The system is mainly meant for location/tracking purposes, but added functionality for transfer of physiological data such as heart rate, core temperature and blood oximetry will likely be implemented in the future. This added monitoring may help in warning the farmer of disease in the flock. This is an important added benefit because sickness is the largest cause of losses, and there is no compensation for animals that die of it.

The proposed system will contain three main units:

- *Base stations* - units strategically located throughout the grazing range. These will communicate with radios on the individual sheep, and also with the system's master control station, which may be simply one of the base stations

---

[1]Official numbers are taken from `www.rovviltportalen.no` and `www.rovbase.no`.

designated as such, or a separate unit at the farm. The base stations will be installed in an elevated position, for instance fastened to trees or radio masts. At the base station, a large power supply such as a lead-acid battery or similar will be available; energy concerns at the base station is therefore not discussed in any detail.

- *Radio collars* - The units attached to the sheep, typically designed as a collar around the sheep's neck. This unit will contain a battery, an antenna and the electronics required to communicate with the base stations.

- *Electronic ear tags* - Very small units attached to the sheep's ear in a fashion similar to that of ID tags. These will take of physiological measurements in the future system. Because of the proximity to bare skin, temperature, optical pulse and oximetry readings will be possible. These units will communicate short-range with the radio collar. The ear tags are considered a future extension in this thesis work and will therefore not be discussed further.

There are several pre-existing systems that utilize a combination of GPS and cellular service to take care of respectively location and communication with a central. There are two main reasons why such a system is unsuitable for this project:

- GPS is power-demanding. Because the sheep are grazing unsupervised on a free range anywhere between 4 and 12 months, the system should be highly energy-efficient to minimize battery changes. Additionally, a larger battery will make the collar heavier, and this weight is limited (especially for lambs).

- Signal coverage: A GPS-based system similar to the one mentioned above was tested in a pioneer project carried out by Trøndelag Forskning og Utvikling in 2010. In their final report they show that the system had none or negligible effects in cutting the loss of animals. They mention technical challenges, mainly the lack of GPS and cellular coverage in significant parts of the grazing range as main causes.[2]

With this in mind, this thesis will investigate alternative methods of location based on a system with dedicated base stations. The main challenge will be the accuracy of the proposed system where price and complexity are limiting factors.

The tracking resolution, determined by the interval between locations is a limiting factor to the battery life. In this project an adjustable frequency of up to 10 positions

FIGURE 1.1: This sheep is outfitted with a GPS-enabled tracking device from Telespor, one of the commercial solutions already available to farmers. Photo taken from `www.viltkamera.no`.

per hour is desirable, which is a very high number compared to existing systems. A high tracking resolution may have numerous benefits:

- Added information of grazing quality, by looking into where the healthiest and heaviest animals graze compared to the others.

- Information about which ewes are keeping their lambs the closest. This is important because an adult sheep may be able to deter smaller predators such as eagles or wolverines, whereas a lamb on its own will be defenseless.

- Alerting the farmers of predator attacks. For example, this could be triggered if many animals start running at the same time.

- Possible deaths: alerting the farmer if the sheep remains still for more than a predetermined amount of time.

- Simplifies gathering the flock at the end of the grazing season. Real-time tracking of the sheep will make it much easier to locate all of them.

1.1.2 Existing systems

Several solutions for tracking animals are commercially available for tracking of both domestic and wild animals. Traditional, inexpensive systems for location include a

radio collar and a hand-held directive antenna. This enables the user to manually determine the bearing at which the transmitter is located. If you have two receivers at known location sufficiently spaced apart, bearings from these two will intersect at the transmitter's location. For stationary antennae, as would be the case with base stations, one would use scanning antenna arrays instead of physically sweeping with a single directional element. For tracking multiple moving targets this quickly evolves into a technically and computationally advanced system.

Another commercial solution uses GPS-receivers on each animal to determine its location, which is in turn reported to a database through available communication channels. A few varieties are mentioned here:

- "Radiobjeller" from Telespor (`www.telespor.no`): GPS positioning with reporting through GSM/GPRS, see Figure 1.1. Battery life: approximately 1000 fixes+reports.

- "Findmysheep" (`www.findmysheep.com`): "E-collars" using GPS positioning and reporting through satellite telephone. Battery life: approximately 600 fixes+reports.

- Lotek GPS collars (`www.lotek.com/gps7000.htm`): GPS positioning with reporting through UHF radio or Argos satellite telephone, see Figure 1.2. Battery life: approximately 2000 fixes/reports.

For the tracking of sheep it a tracking frequency of up to about ten locations per hour is desirable. This means that all of the systems mentioned above would run out of battery in less than two weeks.

1.2   Scope of the project and limitations.

The proposed system will use the low-energy, high-performance transceiver CC1120 from Texas Instruments. The purpose of this thesis work is to compare different methods of radio location, select the one that will work best with the CC1120 and the design specifications, and, if possible, design a system that achieves a high enough accuracy to track sheep in mountain and forest areas. Ideally to the extent where real-time tracking information can be brought out in the field either to aid in locating the animals.

FIGURE 1.2: Three different sizes of radio collars from Lotek, each with different
battery life and functionality. Photo taken from `www.lotek.com`.

1.2.1   Design guidelines

The precision with which the sheep need to be located will naturally be dependent on
the type of terrain in the grazing range. In this thesis work a maximum acceptable
limit is set at a positioning error of 100 m. Errors of this magnitude will allow for
location in open areas, but in dense forest or hilly surroundings, an error as small
as 20 m may still result in a tedious search before the sheep is found.

Another constraint is the maximum distance at which the radios need to operate.
For the sake of this thesis it is assumed that the transmitter is never further away
from any base station than 5 km. This will define the *region of interest* (RoI) as
referred to in accuracy estimates later on, as well as the maximum spacing between
the base stations when the base station network is deployed in the finished system.

The reason for researching a system based on a Sub-GHz transceiver in a base station
network is to avoid dependency on the GPS system as well as GSM/UMTS mobile
cellular networks. However, in the implementation of the base stations, a GPS
receiver will be included. This is to provide an accurate time/frequency standard
for the base stations, on which the propagation time-based location methods are
especially dependent. The base stations will have a much higher battery capacity

Receiver sensitivity	At 1.2 kbps	−123 dBm
	At 50 kbps	−110 dBm
	Using built-in coding gain	−127 dBm
Current consumption	Rx Sniff Mode	2 mA
	Rx Low-power Mode	17 mA (peak)
	Rx High-performance mode	22 mA (peak)
	Tx @ 14 dBm output	45 mA
	Power Down	0.3 µA
Supply voltage	Min–Max	2.0–3.6 V

TABLE 1.1: Some key figures from the CC1120 datasheet.

than the radio collars, and they can be positioned to ensure that they get GPS or cellular signal coverage, so this should not be a concern in the system design.

1.2.2 The CC1120 transceiver

The CC1120 was chosen because it is a high-performance energy efficient transceiver specifically designed for very low power applications. All filters are built-in, reducing the complexity of the system. Because it is controlled over an SPI interface, only a microcontroller and a minimum of external passive components are required to operate it. A few key characteristics from the datasheet of the CC1120 are reproduced in Table 1.1. More details can be found in Appendix D.[2]

1.2.3 Frequency use regulations

The Post and Telecommunication Authority (PTA) regulates all radio use in Norway. In their rules[3] they list a host of frequency bands where transmission for specific purposes are permitted without the need for per-instance transmission permits. Because the finished system is meant to be sold to farmers all over the country, it needs to operate within these regulations. The radio location and tracking system proposed in this thesis is best covered by §30: Peileutstyr (Homing equipment) no. (4), which allows the free use of radio equipment as part of tracking systems within the following restrictions:

---

[2]The appendix contains an excerpt of the full datasheet, which is available at `http://www.ti.com/lit/gpn/cc1120`.

[3]FOR 2012-01-19 nr 77: Forskrift om generelle tillatelser til bruk av frekvenser (fribruksforskriften)

- Frequency band: 169.000 MHz to 169.750 MHz

- Channel separation: 12.5 kHz or 25 kHz. A maximal channel bandwidth of 50 kHz is permitted if the centre frequency is 169.375 MHz.

- Maximum irradiated power: 500 mW E.R.P. (effective radiated power)

- Maximum transmission time occupancy $< 1\,\%$, i.e. less than 36 s/h

Chapter 2

Theoretical Background

This chapter will introduce the principles behind various methods of using radio waves to locate a transmitter. Mathematical details around each one will be presented, as well as methods of determining the expected accuracy in each case.

Four methods will be compared with respect to their suitability for the purpose of tracking sheep on the open range.

2.1 Radio-based positioning

Radio waves has been used to calculate positions since the beginning of the 20th century, both for navigational purposes and for the location of an unknown transmitter. The simplest form of radio location is called *radio direction finding* (RDF) which involves determining the bearing of a transmitter relative to at least two receivers at known locations and then using basic geometry to calculate the transmitter's position. This technique has been in use since before World War I, and is still used in some applications today, although mainly as an alternative to newer systems such as the LORAN-C navigation system and the more recent GPS satellite navigation.

More complex methods of radio location, based on distance or difference-of-distance measurements rather than bearings, have since been developed, each one with its own benefits and drawbacks.

2.1.1   Radio location

The use of radio waves to determine an unknown position is known as radio location, and can be done in either active or passive mode. An example of passive radio location is RADAR; transmitting radio waves and picking up the reflection from targets which do not necessarily transmit anything of their own. For the scope of this project, only the active form of radio location is of interest. Any form of active radio location involves at least one transmitter and one receiver communicating.

In this project, a set of receivers at known, fixed locations will be referred to as base stations, and each transmitter will be at an unknown location, namely attached to the sheep. With this set-up, there are several techniques that can be used to locate the transmitters. Common for all of the techniques is that once a transmission is picked up by a base station, a so-called LoP (locus of positions) can be calculated, typically defined by bearing or distance from the base station to the transmitter. This locus is the set of all points the transmitter may be located at, limited by the bearing or distance data. In a 2-dimensional plane, these LoPs are lines, curved or straight, and by combining data from base stations at different locations, the LoPs will ideally all intersect at the actual transmitter position, i.e. the one point that simultaneously satisfies the calculations done at each base station.

There are three main techniques for accomplishing this:

- *Triangulation:* If the *direction of arrival* (DoA) of the signal coming from a transmitter can be estimated at the base station, it will indicate the bearing of the transmitter relative to that base station. This means that the LoP in this case is the straight line going from the base station through the transmitter. As there is no information of the distance betweeen them, the LoP extends to infinity, or as far as the maximum range of the system allows it to. If a second bearing is obtained from a different base station, the two LoPs will be intersecting at the transmitter's position, as shown in Figure 2.1. With these two angles and the distance between the two base stations (the *baseline*), calculation of the length of the last two "legs" of the triangle is easily done using trigonometric rules.

- *Circular Trilateration:* If, instead of angle, the *distance* between the base station and the transmitter can be estimated, the LoP becomes a circle, hence the name circular trilateration. This circle is centred at the base station, its radius

equal to the estimated distance. If a second base station also has a distance estimate, these two circles, or LoPs, will have either two intersections or one point of tangency if the transmitter is equidistant to the two base stations. This means that generally three independent distance estimates are needed to get a unique solution for the location. The distances can be estimated based on the signal's time of flight (ToF) or the received signal strength at the base station granted the transmitter's power is known.

- *Hyperbolic Trilateration:* A third technique is to use, instead of absolute distances, the *difference* in distances betweeen the transmitter and two base stations. This difference can be calculated without knowledge of the time at which the signal is transmitted, only its time difference of arrival (TDoA) at two different base stations. The time difference is proportional to the distance difference with a proportionality constant equal to the propagation speed. The LoP is represented by all points having the estimated difference in distance to the two base stations. This is the definition of a *hyperbola.*

(A) Triangulation.

(B) Circular trilateration.

(C) Hyperbolic trilateration.
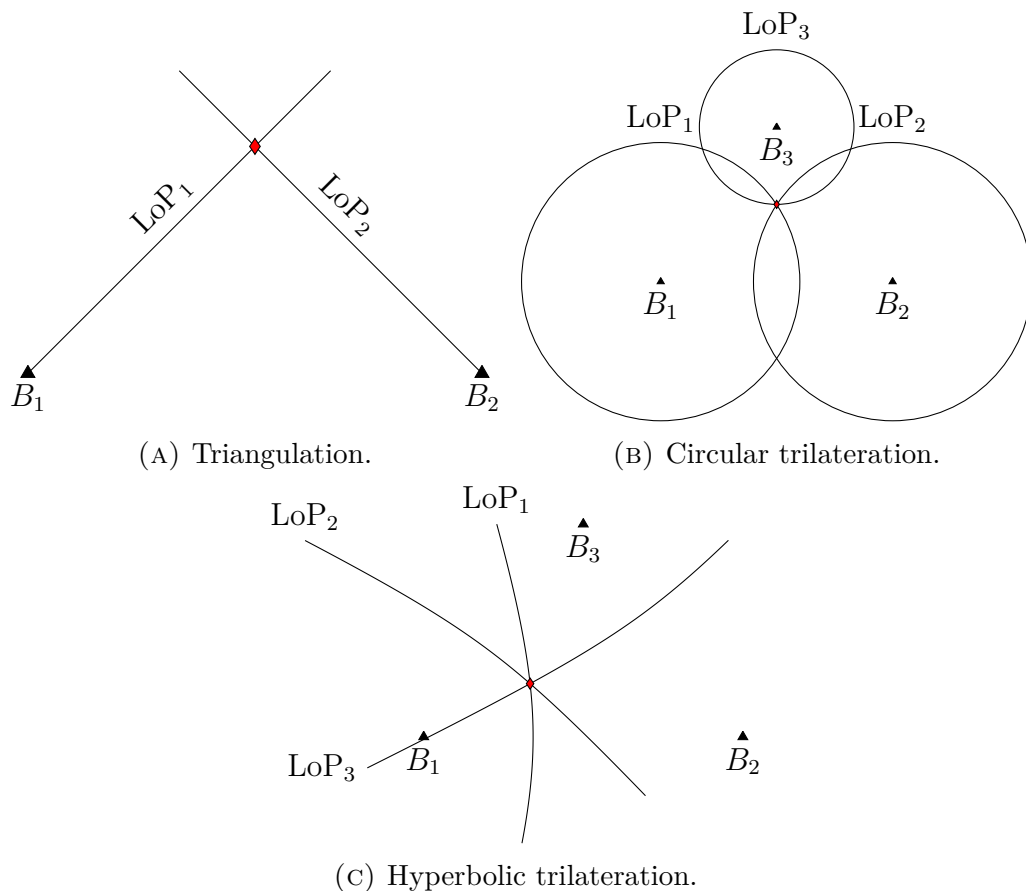
FIGURE 2.1: Different techniques of radio location. The red diamond indicates the transmitter's position.

For all three techniques mentioned above, the estimates done in the base stations are in reality imperfect. The error, whether it is deviation in a DoA estimate or delays and inaccuracies in time-related measurements, distorts the LoPs. This means that the intersection between them is no longer a single point, and not even necessarily at the transmitter's location. If the error is estimated and taken into account, the resulting LoPs will change from lines into areas where the transmitter is likely to be located given the current information. Clean intersections between LoPs will be turned into areas of intersection, the sizes of which depend both on the error's magnitude and the transmitter's position relative to the base stations.

Figures 2.2 through 2.4 show how this error results in areas of uncertainty surrounding the actual transmitter position. The blue lines represent the offset LoPs that may result given an interval for the error. The red lines show the LoPs without measurement errors, i.e. the ones that intersect precisely at the transmitter's position (red diamond).
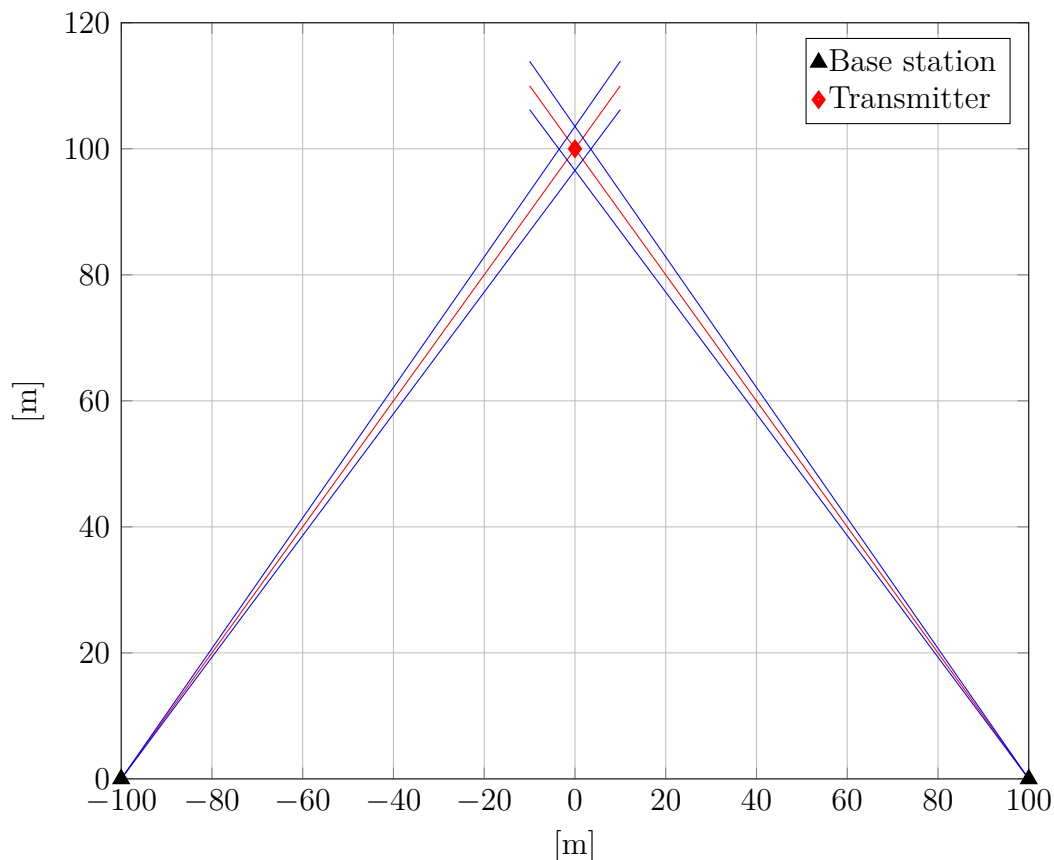
FIGURE 2.2: Triangulation with an angular uncertainty of $\pm 1°$ (blue lines).
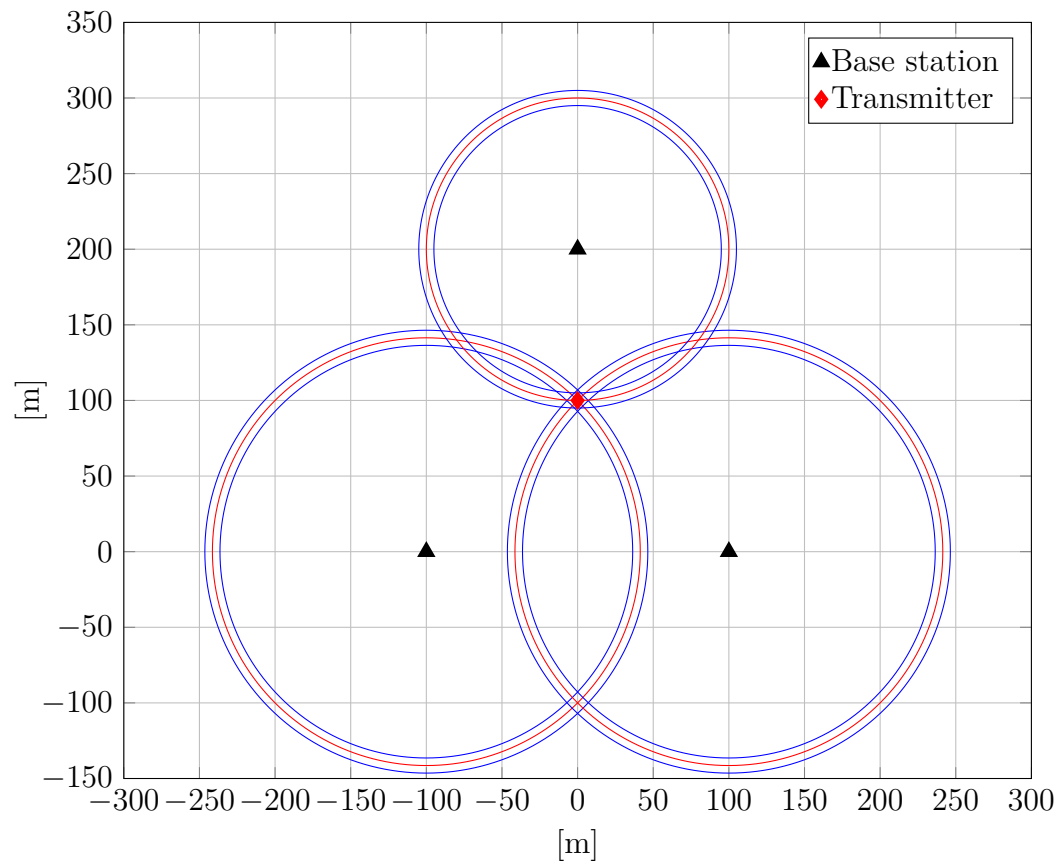
FIGURE 2.3: Circular trilateration with a ranging uncertainty of $\pm 5m$ (blue lines).
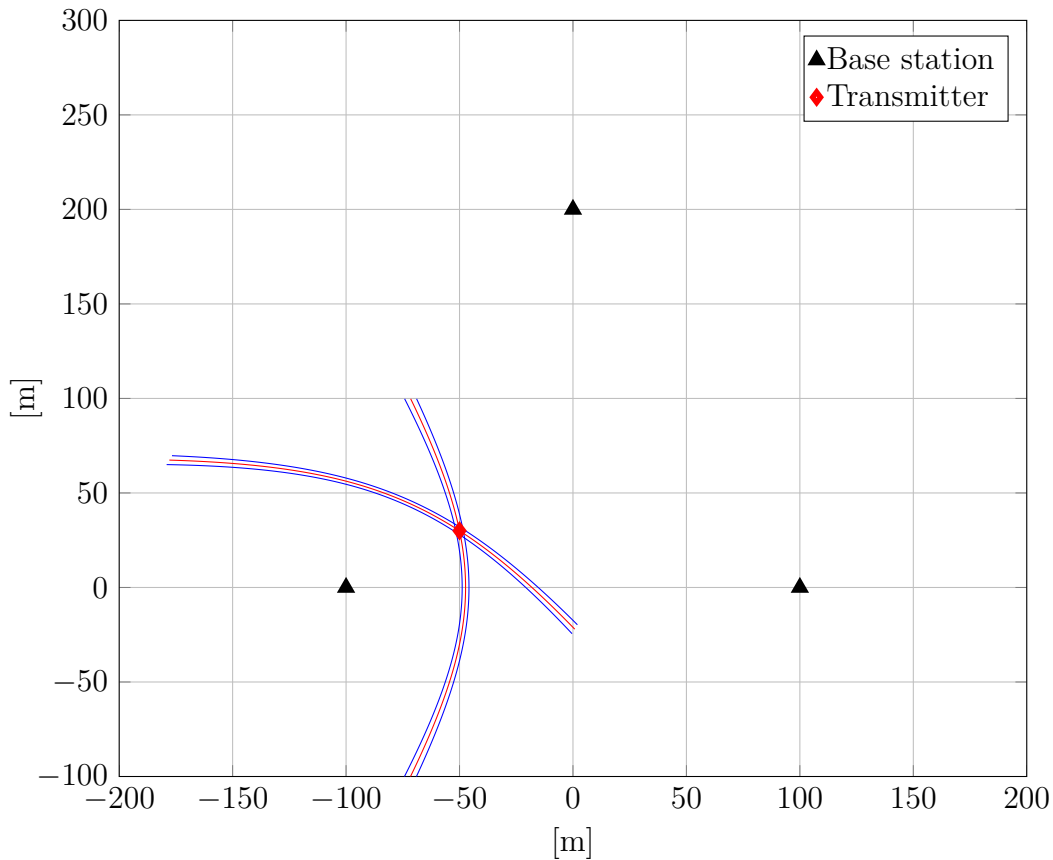
FIGURE 2.4: Hyperbolic trilateration with a timing uncertainty of $\pm 10ns$, corresponding to $\pm 3m$ (blue lines).

2.1.2 Geometric dilution of precision

As mentioned in Chapter 2.1.1, the various measurement errors are not the only factors determining the size of the areas of intersection, it is also affected by the geometry between the transmitter and base stations. Figure 2.5 shows a clear case of how the transmitter's position relative to the two base stations causes a difference in the size of the area of intersection between the two LoPs.

This phenomenon is called *geometric dilution of precision* or GDoP for short and is an important factor in analyzing data from the base stations. When faced with a choice between more than the minimum number of base stations required to calculate a transmitter's position, it would often be best to select the basestations that achieve the lowest GDoP. For every position estimate that is made, a GDoP value should also be calculated as a measure of the quality of that particular position.
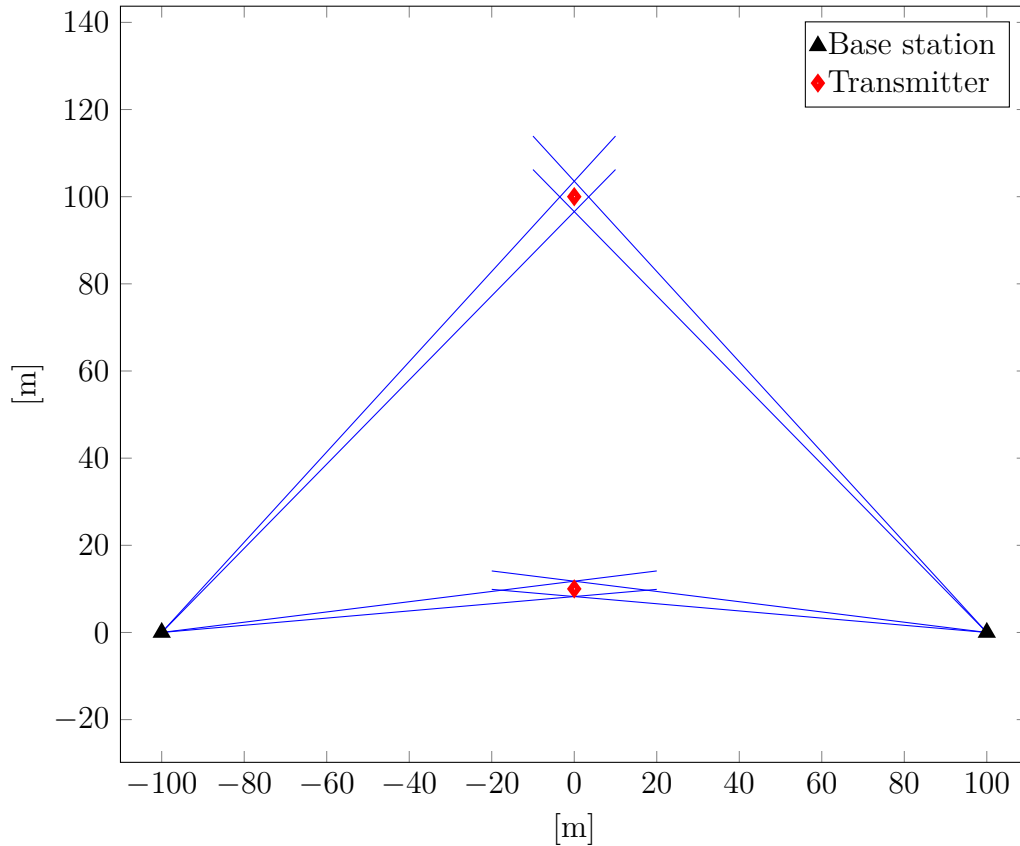
FIGURE 2.5: Example of good and bad geometric dilution of precision (GDoP) when triangulating. The transmitter in (0,100) has low GDoP while the one in (0,10) has high GDoP resulting in a larger area of intersection. Note that both cases have the same angular inaccuracy.

2.2 Circular trilateration in two dimensions

Figure 2.6 shows a typical trilateration problem for $n = 3$ fixed nodes (the base stations) and one unknown node, the transmitter. The following nomenclature will be used to describe positions and distances throughout this chapter:

$$n : \text{The total number of base stations}$$

$$B_i(x_i, y_i) : \text{Base station } i \text{ with coordinates } (x_i, y_i)$$

$$P(x, y) : \text{The transmitter at unknown coordinates } (x, y)$$

$$r_i \text{ [m]} : \text{The range between base } i \text{ and the transmitter}$$

$$d_{i,j} \text{ [m]} : \text{The distance between two base stations } B_i \text{ and } B_j$$
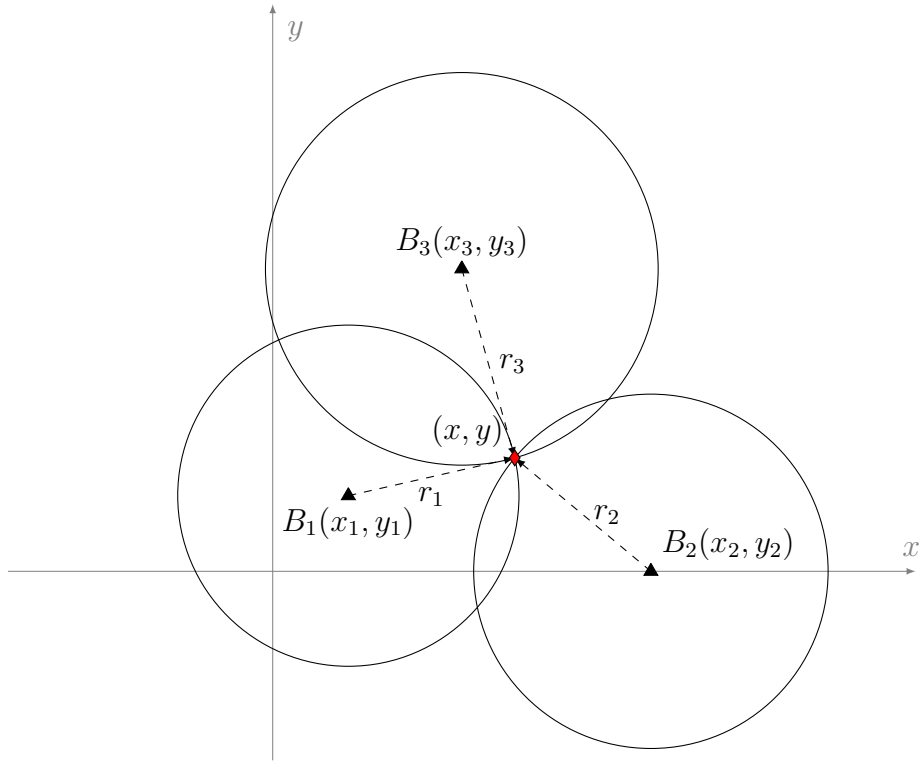
FIGURE 2.6: Circular trilateration with $n = 3$ base stations and error-free distance knowledge.

For each base station, a circular *locus of positions* (LoP) is given by:

$$(x - x_i)^2 + (y - y_i)^2 = r_i^2, \quad (i = 1, 2, \ldots, n) \tag{2.1}$$

The positioning problem consists of finding the point (x, y) that simultaneously satisfies these equations, i.e. the point where distances from the transmitter to each base station i equals r_i. This amounts to finding the intersection of at least three circles, as shown in Figure 2.6. Intuitively, the position is calculated by solving the n equations (2.1) simultaneously for (x, y). However, doing so results in a non-linear system of that is not easily solved.

To simplify things, the equations may be linearised as shown in the following section. This reduces the problem to that of finding an intersection of two or more lines, which will yield the exact position when distance measurements r_i are error-free.

Otherwise, if r_i are estimations of the true distances, the linearised equation set will not have a direct solution, and some form of approximation will have to be made.

2.2.1 Linearisation of the problem

Following the method described in [3], the equation set (2.1) is linearised by using the j'th equation as a linearisation tool. By adding and subtracting x_j and y_j in (2.1) we get:

$$(x - x_j + x_j - x_i)^2 + (y - y_j + y_j - y_i)^2 = r_i^2 \quad (i = 1, 2, \ldots, j-1, j+1, \ldots, n) \quad (2.2)$$

By multiplying through and regrouping terms, this can be written as:

$$
\begin{aligned}
(x - x_j)(x_i - x_j) &+ (y - y_j)(y_i - y_j) \\
&= \frac{1}{2} \left[(x - x_j)^2 + (y - y_j)^2 - r_i^2 + (x_i - x_j)^2 + (y_i - y_j)^2 \right] \\
&= \frac{1}{2} \left[r_j^2 - r_i^2 + d_{i,j}^2 \right]
\end{aligned} \quad (2.3)
$$

Where

$$d_{i,j} = \sqrt{(x_i - x_j)^2 + (y_i - y_j)^2} \quad (2.4)$$

Now, x_i, y_i, x_j, y_j and $d_{i,j}$ are known variables, and r_i, r_j are either known exact or estimated. Note that $(x - x_j), (y - y_j)$ signifies the transmitter's position relative to base station j.

It is arbitrary which value is selected for j, e.g. setting $j = 1$ leads to a set of $n - 1$ linear equations given by:

$$(x - x_1)(x_i - x_1) = \frac{1}{2} \left[r_1^2 - r_i^2 + d_{i,1}^2 \right] \quad (i = 2, 3, \ldots, n) \quad (2.5)$$

Written in matrix form, this is equivalent to:

$$\mathbf{A}\vec{x} = \vec{b} \quad (2.6)$$

Where

$$
\mathbf{A} = \begin{bmatrix} x_2 - x_1 & y_2 - y_1 \\ x_3 - x_1 & y_3 - y_1 \\ \vdots & \vdots \\ x_n - x_1 & y_n - y_1 \end{bmatrix}, \quad
\vec{x} = \begin{bmatrix} x - x_1 \\ y - y_1 \end{bmatrix}, \quad
\vec{b} = \frac{1}{2} \begin{bmatrix} r_1^2 - r_2^2 + d_{2,1}^2 \\ r_1^2 - r_3^2 + d_{3,1}^2 \\ \vdots \\ r_1^2 - r_n^2 + d_{n,1}^2 \end{bmatrix}
$$

This system has $n-1$ independent equations, so if the distances r_i are accurate, the equation set may be solved by picking 3 base stations leading to two equations in two unknowns x and y which are easily solved for by any technique for simultaneous equations, e.g.:

$$\vec{x} = \mathbf{A}^{-1}\vec{b} \tag{2.7}$$

However, because the distance estimates will be imperfect in any real-world application, this solution will not be accurate. Therefore it would be an improvement to use a method capable of including more than three base stations to make the solution progressively better. One such method is the *least squares* approximation.

2.2.2 Linear least squares approximation

One method for estimating a solution (x, y) of (2.6) is the *linear least squares* approximation. Let the *residual*, the error in the approximated solution $\vec{x}$ be denoted by $\vec{\Delta}$. The sum of squared errors may then be written as:

$$SSE = \vec{\Delta}^\top\vec{\Delta} = (\vec{b} - \mathbf{A}\vec{x})^\top(\vec{b} - \mathbf{A}\vec{x}) \tag{2.8}$$

Minimizing this sum, i.e. setting

$$\frac{\partial SSE}{\partial \vec{x}} = -\mathbf{A}^\top\vec{b} + (\mathbf{A}^\top\mathbf{A})\vec{x} = 0 \tag{2.9}$$

results in the *normal equations*, as detailed in [4].

$$(\mathbf{A}^\top\mathbf{A})\vec{x} = \mathbf{A}^\top\vec{b} \tag{2.10}$$

If $(\mathbf{A}^\top\mathbf{A})$ is non-singular, this equation set may be solved by:

$$x = (\mathbf{A}^\top\mathbf{A})^{-1}\mathbf{A}^\top\vec{b} = \mathbf{A}^\dagger\vec{b} \tag{2.11}$$

Where $\mathbf{A}^\dagger$ is the *Moore-Penrose pseudo-inverse* of $\mathbf{A}$. [5]

If $\mathbf{A}^\top\mathbf{A}$ is singular, close to singular or ill-conditioned, the pseudo-inverse $\mathbf{A}^\dagger$ must be calculated by either *QR decomposition* or *singular value decomposition*[4].

- *QR-decomposition* entails finding matrices $\mathbf{Q}$ and $\mathbf{R}$ such that $\mathbf{A} = \mathbf{QR}$ where $\mathbf{Q}$ is an orthogonal matrix, i.e. $\mathbf{Q}^\top\mathbf{Q} = \mathbf{I}$ and $\mathbf{R}$ is upper-diagonal, i.e. all

elements in $\mathbf{R}$ below the main diagonal are zero. This transforms the problem into:

$$\mathbf{R}\vec{x} = \mathbf{Q}^\top \vec{b} \Rightarrow \vec{x} = \mathbf{R}^{-1}\mathbf{Q}^\top \vec{b} \tag{2.12}$$

which is easily solved because $\mathbf{R}$ is upper triangular.

- *Singular value decomposition* decomposes $\mathbf{A}$ such that $\mathbf{A} = \mathbf{U}\mathbf{\Sigma}\mathbf{V}^\top$ where $\mathbf{A}$ is a $n \times 2$ (for two dimensions) real matrix, $\mathbf{U}$ is a $n \times n$ orthogonal matrix, $\mathbf{\Sigma}$ is a $n \times 2$ diagonal matrix and $\mathbf{V}^\top$ is a 2×2 orthogonal matrix. With this decomposition, the pseudoinverse and consequently the least squares solution given by:

$$\mathbf{A}^\dagger = \mathbf{V}\mathbf{\Sigma}^\dagger\mathbf{U}^\top \Rightarrow \vec{x} = \mathbf{V}\mathbf{\Sigma}^\dagger\mathbf{U}^\top \vec{b} \tag{2.13}$$

Using MATLAB, any linear equation set on the form of (2.6) may be solved by using the backslash operator: `x = A\b`. If the system is fully determined, i.e. $\mathbf{A}$ is $n \times n$ and non-singular, MATLAB will return the unique solution as given by equation (2.7). If the system is under- or over determined, MATLAB will compute a linear least squares approximation using the QR decomposition as described above.

2.2.3 Non-linear least squares approximation

A third approach when there is no single point of intersection between the LoPs is to use an iterative method to minimize the squared error in distances. The Gauss-Newton algorithm is one such method, and can be applied to the trilateration problem as shown here:

For any point (x, y) the true distance to base station i is given by

$$r_i = \sqrt{(x - x_i)^2 + (y - y_i)^2} \tag{2.14}$$

Given a set of estimated or measured distances $\hat{r}_i$ from each base station, the sum of squared distance residuals $f_i(x, y)$ is:

$$SSE(x, y) = \sum_{i=1}^{n} f_i(x, y)^2 = \sum_{i=1}^{n} (r_i - \hat{r}_i)^2 = \sum_{i=1}^{n} \left(\sqrt{(x - x_i)^2 + (y - y_i)^2} - \hat{r}_i \right)^2 \tag{2.15}$$

The optimal position (x, y) can now be found by minimizing $SSE(x, y)$. To do this, the derivative is set to zero:

$$\begin{bmatrix} \frac{\partial SSE}{\partial x} \\ \frac{\partial SSE}{\partial y} \end{bmatrix} = \begin{bmatrix} 2\sum_{i=1}^{n} f_i \frac{\partial f_i}{\partial x} \\ 2\sum_{i=1}^{n} f_i \frac{\partial f_i}{\partial y} \end{bmatrix} = 2\mathbf{J}^{\top} \vec{f} = 0 \tag{2.16}$$

Where $\mathbf{J}$ is the *Jacobian* matrix of the function set f_i:

$$\mathbf{J} = \begin{bmatrix} \frac{\partial f_1}{\partial x} & \frac{\partial f_1}{\partial y} \\ \vdots & \vdots \\ \frac{\partial f_n}{\partial x} & \frac{\partial f_n}{\partial y} \end{bmatrix}, \quad \vec{f} = \begin{bmatrix} f_1 \\ \vdots \\ f_n \end{bmatrix}$$

The Gauss-Newton algorithm is a modified version of Newton's method optimized for the minimization of a sum of squares. It eliminates the need for second-order derivatives, thereby simplifying calculations.[6, Chap. 9] Defining the position vector $\vec{x} = (x, y)^{\top}$, the iterative method is given by:

$$\vec{x}_{k+1} = \vec{x}_k - (\mathbf{J}_k^{\top} \mathbf{J}_k)^{-1} \mathbf{J}_k^{\top} \vec{f_k} = \vec{x}_k - \mathbf{J}_k^{\dagger} \vec{f_k} \tag{2.17}$$

Where $\mathbf{J}_k, \vec{f_k}$ denotes the Jacobian matrix and the set of residuals computed at $\vec{x}_k$, and $\mathbf{J}^{\dagger}$ denotes the Moore-Penrose pseudoinverse of $\mathbf{J}$. The initial position $\vec{x}_1$ can for instance be set equal to the result of the linear least square approximation from the previous section. Expanding $f_i(x, y)$ and writing out the matrices yields:

$$\mathbf{J}^{\top}\mathbf{J} = \begin{bmatrix} \sum_{i=n}^{n} \frac{(x-x_i)^2}{r_i^2} & \sum_{i=n}^{n} \frac{(x-x_i)(y-y_i)}{r_i^2} \\ \sum_{i=n}^{n} \frac{(x-x_i)(y-y_i)}{r_i^2} & \sum_{i=n}^{n} \frac{(y-y_i)^2}{r_i^2} \end{bmatrix}, \quad \mathbf{J}^{\top}\vec{f} = \begin{bmatrix} \sum_{i=n}^{n} \frac{(x-x_i)(r_i-\hat{r}_i)}{r_i} \\ \sum_{i=n}^{n} \frac{(y-y_i)(r_i-\hat{r}_i)}{r_i} \end{bmatrix}$$

A MATLAB function that implement this method and calculates a solution for position x and y, given base station positions and respective range estimates has been written as part of this thesis work, and can be found in Appendix C.

2.3   Hyperbolic trilateration in two dimensions

If the absolute distance between a base station and the transmitter is unknown , a possibility is to use the difference between distances for a *pair* of base stations, as discussed in Section 2.1.1. A locus of all positions in the plane satisfying a constant difference of distances to two *foci* (the base stations) is described by a hyperbola.

Using the same nomenclature as earlier, Figure 2.7 shows a typical case of hyperbolic trilateration. In the following section, let the distance difference be denoted by:
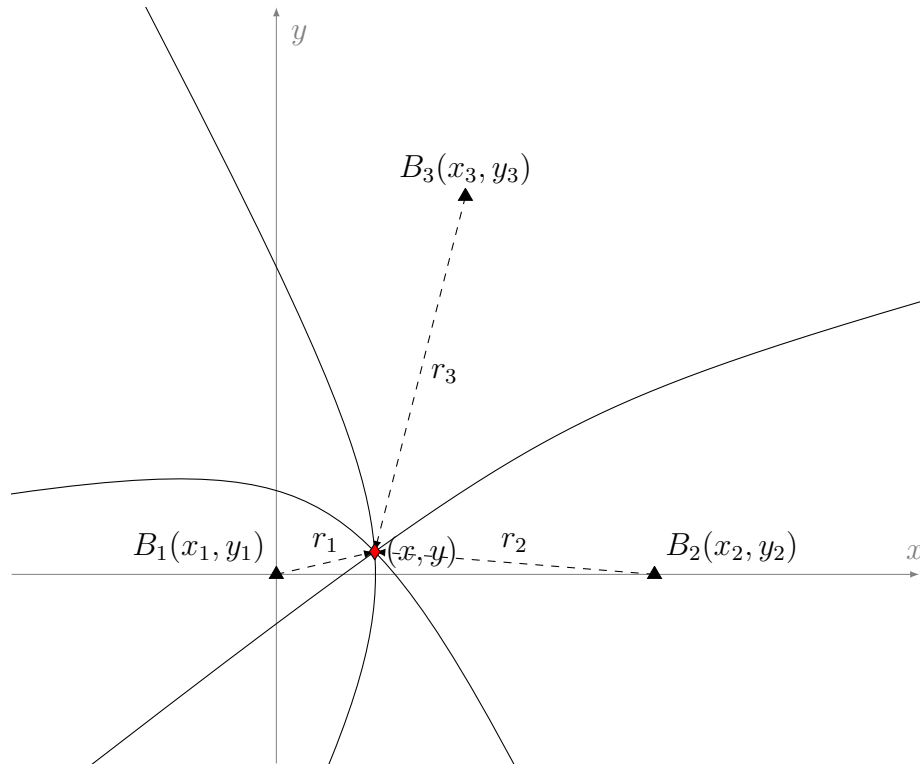
FIGURE 2.7: Hyperbolic trilateration for $n = 3$ bases and error free distance difference knowledge.

$$r_{i,j} = r_i - r_j = c(t_i - t_j) = c\tau_{i,j} \tag{2.18}$$

Where c is the signal propagation speed and t_i and t_j are the time of reception at base station i and j, respectively. The value $\tau_{i,j} = t_i - t_j$ is the *time difference of arrival* (TDoA). If the total number of base stations is n, there are $M = \binom{n}{2}$ different TDoAs. To eliminate redundancy and calculate the optimal set of TDoAs in the case where noise is present in the time measurements, Hahn and Tretter's [7] method can be used. This method works by calculating the Gauss-Markov weighted estimates for each TDoA as referenced to the first transmitter, $\tau_{i,1} = t_i - t_1, \quad (i = 2, 3, \ldots, n)$ based on the TDoA's for all possible base station pairs. The optimal estimate for the TDoA between base stations i and j is then given by

$$\tau_{i,j} = \tau_{i,1} - \tau_{j,1}, \quad (i,j = 2, 3, \ldots, n) \tag{2.19}$$

These TDoA estimates are optimal in the sense that the *Cramér-Rao lower bound* (CRLB) is achievable.

Using the distance difference estimates, the LoP for a base station pair B_i, B_j is then the locus of all points (x, y) satisfying:

$$\sqrt{(x - x_i)^2 + (y - y_i)^2} - \sqrt{(x - x_j)^2 + (y - y_j)^2} = r_{i,j} \qquad (2.20)$$

This is a set of $n - 1$ non-linear equations in two unknowns (x, y). Solving this equation set directly is not feasible; a linearisation is needed to solve the problem.

2.3.1 Linearisation of the problem

The linearisation may be done by applying a Taylor series expansion of (2.20) and discarding all terms of second order or higher as shown in [8]. Based on an initial position estimate (x_0, y_0), an iterative approach should converge against a solution (x, y). However, convergence is not guaranteed, and this method requires an initial position that is somewhat accurrate. It is also computationally intensive.

An alternative approach is linearisation by selecting the j-th base station as a linearisation tool. In the following, index $j = 1$ is arbitrarily chosen. Isolating r_i in (2.18) and squaring both sides gives:

$$r_i^2 = (r_{i,j} + r_j)^2 = r_{i,j}^2 + 2r_{i,j}r_j + r_j^2, \quad (i = 1, 2, \ldots, j - 1, j + 1, \ldots, n) \qquad (2.21)$$

Expanding the definition of r_i:

$$r_i^2 = (x - x_i)^2 + (y - y_i)^2 = K_i - 2x_i x - 2y_i y + x^2 + y^2, \quad \text{where } K_i = x_i^2 + y_i^2 \quad (2.22)$$

and inserting back into (2.21) yields:

$$r_{i,j}^2 + 2r_{i,j}r_j + r_j^2 = K_i - 2x_i x - 2y_i y + x^2 + y^2 \qquad (2.23)$$

Subtracting r_j^2 as given by (2.22) from (2.23) eliminates the square terms of x and y and results in:

$$r_{i,j}^2 + 2r_{i,j}r_j = K_i - K_j - 2(x_i - x_j)x - 2(y_i - y_j)y, \quad (i = 1, 2, \ldots, j - 1, j + 1, \ldots, n) \qquad (2.24)$$

This is now a set of $n - 1$ linear equations in 3 unknowns r_j, x and y. Rearranging variables and translating the set to matrix form, setting $j = 1$, gives:

$$\mathbf{A}\vec{x} = \vec{b} \tag{2.25}$$

where:

$$\mathbf{A} = - \begin{bmatrix} (x_2 - x_1) & (y_2 - y_1) & r_{2,1} \\ \vdots & \vdots & \vdots \\ (x_n - x_1) & (y_n - y_1) & r_{n,1} \end{bmatrix} \quad \vec{x} = \begin{bmatrix} x \\ y \\ r_1 \end{bmatrix} \quad \vec{b} = \frac{1}{2} \begin{bmatrix} r_{2,1} - K_2 + K_1 \\ \vdots \\ r_{n,1} - K_n + K_1 \end{bmatrix}$$

2.3.2   Solution of the linearised problem

The equation set (2.25) is easily solved when $n = 4$ using any well-known method such as Gaussian elimination, or by inversion of the coefficient matrix: $\vec{x} = \mathbf{A}^{-1}\vec{b}$. When the system is over-determined, $n > 4$, an approximate solution can be calculated by first solving for x and y as functions of r_1, then substituting the calculated least square solution for r_1 back into (2.25) to get values for x and y. This method is called the *spherical interpolation* (SI) solution[9]. It provides a solution that minimizes the squared error in the position estimate, but cannot make use of additional measurements to improve the accuracy of the solution.

In [10], Chan and Ho improves on Fang's algorithm[11] so that it can use additional measurements when $n > 3$ to provide a more accurate solution. It also provides a closed-form solution for the case of $n = 3$ TDoA measurements. The remainder of this section is a summary of that algorithm with base stations at arbitrary coordinates.

$$r_j = \sqrt{(x - x_j)^2 + (y - y_j)^2} \tag{2.26}$$

By utilising the fact that r_j is not actually an independent variable of the equation set (2.25), but rather a nonlinear function of x and y given by (2.26) an analytical solution for the case where $n = 3$ can be worked out.

First, rewrite (2.25) for x and y as functions of r_1:

$$- \begin{bmatrix} (x_2 - x_1) & (y_2 - y_1) \\ (x_3 - x_1) & (y_3 - y_1) \end{bmatrix} \begin{bmatrix} x \\ y \end{bmatrix} = \begin{bmatrix} r_{2,1}r_1 + \frac{1}{2}(r_{2,1} - K_2 + K_1) \\ r_{3,1}r_1 + \frac{1}{2}(r_{3,1} - K_3 + K_1) \end{bmatrix} \tag{2.27}$$

Next, solve for x and y expressed by r_1:

$$\begin{bmatrix} x \\ y \end{bmatrix} = - \begin{bmatrix} (x_2 - x_1) & (y_2 - y_1) \\ (x_3 - x_1) & (y_3 - y_1) \end{bmatrix}^{-1} \begin{bmatrix} r_{2,1}r_1 + \frac{1}{2}(r_{2,1} - K_2 + K_1) \\ r_{3,1}r_1 + \frac{1}{2}(r_{3,1} - K_3 + K_1) \end{bmatrix} \qquad (2.28)$$

Next, substitute this solution for x and y into equation (2.22). This yields a quadratic equation in r_1. Finally, inserting the positive solution for r_1 back into (2.28) solves the trilateration problem for the transmitter's position (x, y). In some cases, the quadratic equation may have two positive roots, giving two possible solutions. This ambiguity may be avoided by restricting the solution to a *region of interest*, e.g. a maximum distance away from the previous position or a maximum distance away from any base station.

See Appendix B for a MATLAB implementation of Chan's method that was developed as part of the thesis work.

2.4   Accuracy for various methods of location

Four different methods of radio location will be analysed in this thesis and compared with respect to their suitability for this project. The analysis will be based on finding out what measurement precision that may be achieved within reasonable limits on price and complexity, and further investigating if locating sheep on the open range would be possible with that precision.

The design specifications demand that location will be possible at ranges up to 5 km between sheep and base station. Factors that affect measurements and communication include the topography of the area, vegetation, weather and other atmospheric conditions such as humidity and temperature.

The four methods that will be compared are:

- *Circular trilateration based on received signal strength (RSSI):*

  This method will use signal strength measurements at each base station as a measure of how far away the transmitter is. The CC1120 transceivers are pre-equipped with everything that is necessary to measure signal strength, or *received signal strength indicator* (RSSI). Given distance estimates for at

least three different base stations at known locations, the positioning of the transmitter is a simple case of circular trilateration, see Chapter 2.1.1.

- *Triangulation with directional antennas or arrays:*

  This method is classic triangulation where the bearing from at least two base stations to the transmitter is found, see Chapter 2.1.1 for details. To do this, one can either physically rotate an antenna with very high directivity properties and find the peak (or null) direction, or use a scanning phased array with multiple antenna elements.

- *Circular trilateration based on round-trip propagation time:*

  Here, the absolute distance between base station and transmitter is estimated by measuring the time it takes from a packet is transmitted from the base station until an reply is received from the transmitter at the unknown location. This requires that delays at receiver and transmitter due to wake-up time, signal processing and so on is constant, so that the actual propagation time of the radio signal can be calculated. Because the radio waves travel at a, for all practical purposes in this thesis work, constant speed in open air, the distance between the base stations and the transmitters may be directly derived from this time measurement. Repeating the procedure for three different base stations, the trilateration is performed in the same way as for the RSSI-based method.

- *Hyperbolic trilateration based on time difference of arrival:*

  Even if the actual propagation time of the signal from the transmitter to a base station cannot be determined, location may still be possible using *time difference of arrival (TDoA)* measurements. These measurements require all of the base stations to have a synchronised clock. The time difference is then found by transmitting a signal from the unknown position, and comparing the times of arrival for the base stations receiving it. Using at least three base stations yields three different TDoA measurement, which gives three different hyperbolas for the corresponding distance difference. These hyperbolas intersect at the transmitter's position, see Chapter 2.1.1.

2.4.1   The RSSI method

The power incident on a receiver (RX) at a given distance from a transmitter (TX) can be calculated by using the Friis transmission equation.[12, Chap. 2] Ignoring loss factors due to impedance mismatch in the signal path and polarization mismatch between the antennae, its simplified form is:

$$\frac{P_r}{P_t} = \left(\frac{\lambda}{4\pi R}\right)^2 G_t G_r \Rightarrow R = \frac{\lambda}{4\pi}\sqrt{\frac{P_t G_t G_r}{P_r}} \tag{2.29}$$

Where the different quantities are:

$$
\begin{aligned}
R\ [\text{m}] :&\quad \text{the propagation distance between the TX and RX antennae.}\\
P_t, P_r\ [\text{W}] :&\quad \text{power at TX and RX antenna terminals, respectively.}\\
G_t, G_r\ [\text{unitless}] :&\quad \text{Gain in TX and RX antennae, respectively.}\\
\lambda\ [\text{m}] :&\quad \text{Wavelength of radiowave in the propagation medium.}
\end{aligned}
$$

This shows that the received signal power is inversely proportional to the squared distance, which means the distance is a inversely proportional to the square root of the received power.

2.4.1.1   Measurement accuracy

The CC1120 quantifies RSSI in the range from -128 dBm to 127 dBm using a 12 bit two's complement number. The quantisation step size is 0.0625 dBm. [13, chap. 6.9].This means that, ignoring all other errors, the measurements still include a quantisation error on the range: $\Delta_{\text{dB}} \in (-0.03125, 0.03125)$ dBm. Although the quantisation is uniform (constant quantisation step size), because it is performed on the logarithmic dBm-scale the resulting error in the distance estimate will not be uniformly distributed.

The fact that the spatial resolution of the ranging method is dependent on the quantisation step size results in a phenomenon known as *range binning* [14], where in this case the width of each range bin is varying.

The expression for this distance error is calculated by first rewriting equation (2.29) into dB values. The error-free distance estimate R is then given by:

$$R = \frac{\lambda}{4\pi} 10^{\frac{1}{20}(P_{t,\text{dBm}}+G_{t,\text{dB}}+G_{r,\text{dB}}-P_{r,\text{dBm}})} \tag{2.30}$$

Let the distance estimate including the quantisation error be denoted by $\hat{R}$.

$$\hat{R} = \frac{\lambda}{4\pi} 10^{\frac{1}{20}\left(P_{t,\text{dBm}}+G_{t,\text{dB}}+G_{r,\text{dB}}-(P_{r,\text{dBm}}+\Delta_{\text{dB}})\right)} = R \cdot 10^{-\frac{1}{20}\Delta_{\text{dB}}} \tag{2.31}$$

The actual error that is made in the distance estimate is then given by:

$$\Delta_R = \hat{R} - R = R(10^{-\frac{1}{20}\Delta_{\text{dB}}} - 1) \tag{2.32}$$

It is apparent that the error is multiplicative in nature, and that it grows with R. Specifically, inserting for the worst-case values of quantisation errors, the corresponding distance error or range bin width, at a distance R, is given by:

$$\Delta_{\text{dB}} = -0.03125 \qquad \Rightarrow \Delta_R \approx R \cdot 0.0036 \qquad (+0.36\ \%) \tag{2.33}$$

$$\Delta_{\text{dB}} = +0.03125 \qquad \Rightarrow \Delta_R \approx R \cdot (-0.0036) \qquad (-0.36\ \%) \tag{2.34}$$

This means that for distances of around 100 m, the range bin width will be ± 0.36 m, while at 1 km it is ± 3.6 m.

Missing the target by 3.6 m at a distance of 1 km may not seem to hinder the location of sheep, but that is assuming no other error sources affect the RSSI measurement, which is not the case. Systemic errors such as misalignment of the antennas cause polarization losses and is highly likely because one antenna will be fastened to a sheep's collar. Environmental effects on the radio waves such as reflections, scattering and absorption due to topography and vegetation cause measurement errors, as well as multi-path effects such as small-scale channel fading caused by constructive/destructive interference between the main signal and reflected images [15, chap. 2].

Assuming a more realistic total measurement error of ± 1 dBm, the range bin width is now given by

$$\Delta_{\text{dB}} = -1 \qquad \Rightarrow \Delta_R \approx R \cdot 0.1220 \qquad (+12.20\ \%) \tag{2.35}$$

$$\Delta_{\text{dB}} = +1 \qquad \Rightarrow \Delta_R \approx R \cdot (-0.1087) \qquad (-10.87\ \%) \tag{2.36}$$

It is clear that even if the quantizer is uniform so that the quantisation error itself has the same statistic distribution at all signal levels, the impact it makes on the range estimate is greater at large distances because of the logarithmic nature of the dBm scale. This is a highly undesirable property for this system, where distances between transmitter and receiver may be several kilometres.

Using the distance errors from (2.35) for a distance of $R = 5$ km, the range bin becomes:

$$R_{max} = R + 12.87 \ \% = 5000 \cdot (1 + 0.1220) \approx 5610 \text{ m} \qquad (2.37)$$

$$R_{min} = R + 12.87 \ \% = 5000 \cdot (1 - 0.1087) \approx 4457 \text{ m} \qquad (2.38)$$

This results in an uncertainty range of more than a kilometre and is certainly not optimal for locating sheep in mountain/forest areas.

2.4.1.2   Geometric dilution of precision

The RSSI measurements provide a distance measurement with a certain accuracy. Using estimates from three or more base stations at different locations, the transmitter's position may be estimated using circular trilateration algorithms as decribed in Section 2.1.1. The accuracy of this estimate is limited of course by the range binning discussed in the previous section, as well as the geometry between the base stations and the transmitters.

Because the LoPs for circular trilateration are circles, two LoPs will have either two points of intersection or a single point of tangency in the case that the transmitter is located on the line between two base stations and equidistant to both. Assuming this ambiguity has been eliminated using a third LoP, the detailed geometry at the intersecting point is shown in Figure 2.8. In the figure, Δ_{A+}, Δ_{A-} and Δ_{B+} are the maximum distance estimate errors and ϵ_+ and ϵ_- are the resultant positioning errors, i.e. how far from the true position a estimate was, given a positive or negative error, respectively, in the distance estimate. γ is the angle between base station A and B with its vertex at the transmitter's position, often called the *aspect angle*. Assuming that the distance, i.e. the radius of each LoP, is much greater than the radius shift caused by the error, the LoP may be considered linear within a small region of interest. The LoPs, which in reality are circles centred on the base stations, can then be represented by their tangency lines perpendicular to the direction of the
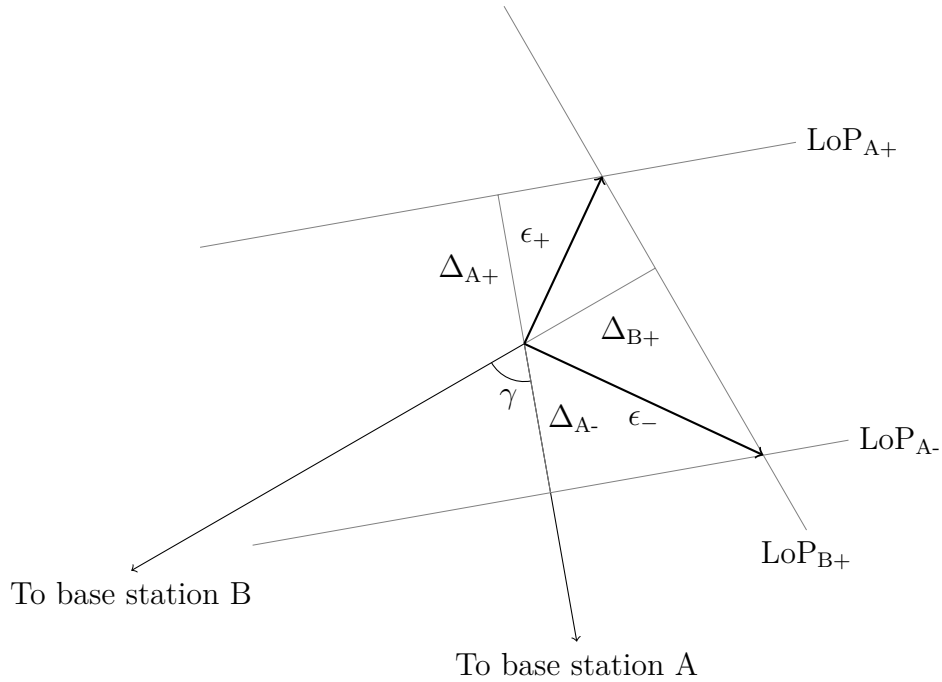
FIGURE 2.8: This figure shows error in position as a consequence of measurement inaccuracy and base station geometry.

base station as seen from the transmitter. The line LoP$_{B-}$, the shift due to a negative distance error in the estimate for base station B, is omitted in the following because it only creates a situation that is a mirror image of the one that is shown.

The magnitude of the positioning error is derived in Forssell [16], and is roughly summarized in equations (2.39) through (2.43).

Assuming that the error in the distance estimate caused by the measurement error is equal in both positive and negative direction, $\Delta_{A+} = \Delta_{A-} = \Delta_A$, a simplification of what is shown by equation (2.35), the errors are given by:

$$\epsilon_+ = \frac{\Delta_A}{\sin\gamma}\sqrt{1 + \left(\frac{\Delta_B}{\Delta_A}\right)^2 - \frac{2\Delta_B}{\Delta_A}\cos\gamma} \qquad (2.39)$$

$$\epsilon_- = \frac{\Delta_A}{\sin\gamma}\sqrt{1 + \left(\frac{\Delta_B}{\Delta_A}\right)^2 + \frac{2\Delta_B}{\Delta_A}\cos\gamma} \qquad (2.40)$$

Furthermore, assuming that the magnitude of the measurement error is the same for base station A and B, $\Delta_A = \Delta_B$, the simplified expression becomes:

$$\epsilon_+ = \frac{\Delta_A}{\sin\gamma}\sqrt{2(1-\cos\gamma)} = \frac{\Delta_A}{\sin\gamma}2\sin\frac{\gamma}{2} = \frac{\Delta_A}{\cos\frac{\gamma}{2}} \tag{2.41}$$

$$\epsilon_- = \frac{\Delta_A}{\sin\gamma}\sqrt{2(1+\cos\gamma)} = \frac{\Delta_A}{\sin\gamma}2\cos\frac{\gamma}{2} = \frac{\Delta_A}{\sin\frac{\gamma}{2}} \tag{2.42}$$

The error is minimised for $\gamma = 90°$ where $\epsilon_+ = \epsilon_- = \Delta_A\sqrt{2}$. Because $\epsilon_- > \epsilon_+$ for $\gamma < 90°$ and vice versa for $\gamma > 90°$, the maximum error may be summarized by:

$$\epsilon_{\max} = \begin{cases} \frac{\Delta_A}{\sin\frac{\gamma}{2}} & \text{for } 0° < \gamma \leq 90° \\ \frac{\Delta_A}{\cos\frac{\gamma}{2}} & \text{for } 90° < \gamma < 180° \end{cases} \tag{2.43}$$

2.4.2   The direction-of-arrival method

In the case of regular triangulation the accuracy is determined by the error made in the *direction-of-arrival* (DoA) estimate. Traditionally, the DoA estimate of a radio wave was found using a rotating antenna with very sharply defined directive properties, commonly a very narrow null in its radiation pattern, and noting at which bearing the signal is detected or lost. Modern systems use multiple antenna elements set up in an array. The directivity of such an array can be manipulated by modifying phase/amplitude parameters for each element. This means that the system driving the array can "scan" through all directions in hardware or software to determine the DoA of an incoming signal.[12, Chap. 16] Commercially available automatic direction finding (ADF) systems for use in e.g. search and rescue missions or navigation such as the Rockwell & Collins SAR-126,[1] or the TD-L1630 from Taiyo Musen[2] both provide a bearing accuracy of better than $\pm 3°$.

2.4.2.1   Measurement accuracy

Given an uncertainty in the DoA estimate, the LoP changes from a line through the transmitter's position to a sector originating from the base station. If the measuring error is denoted in degrees by Δ_{DoA}, the arc length s of this sector at any given

---

[1]http://www.rockwellcollins.com/sitecore/content/Data/Products/Navigation_and_Guidance/Direction-Finding_Equipment/SAR-126_VHF_Direction_Finder.aspx
[2]http://www.taiyomusen.co.jp/pdf/TD-L1630-E.pdf

distance R is given by:

$$s = R \cdot \Delta_{\text{DoA}} \frac{\pi}{180} \tag{2.44}$$

2.4.2.2 Geometric dilution of precision

By assuming that the measurement accuracy is on the order of a few degrees, the LoPs can be approximated as parallel lines. Let $\text{LoP}_{\text{A+}}$ and $\text{LoP}_{\text{A-}}$ represent base station A's shifted LoPs in positive and negative direction, respectively, and $\text{LoP}_{\text{B+}}$ and $\text{LoP}_{\text{B-}}$ those of base station B.
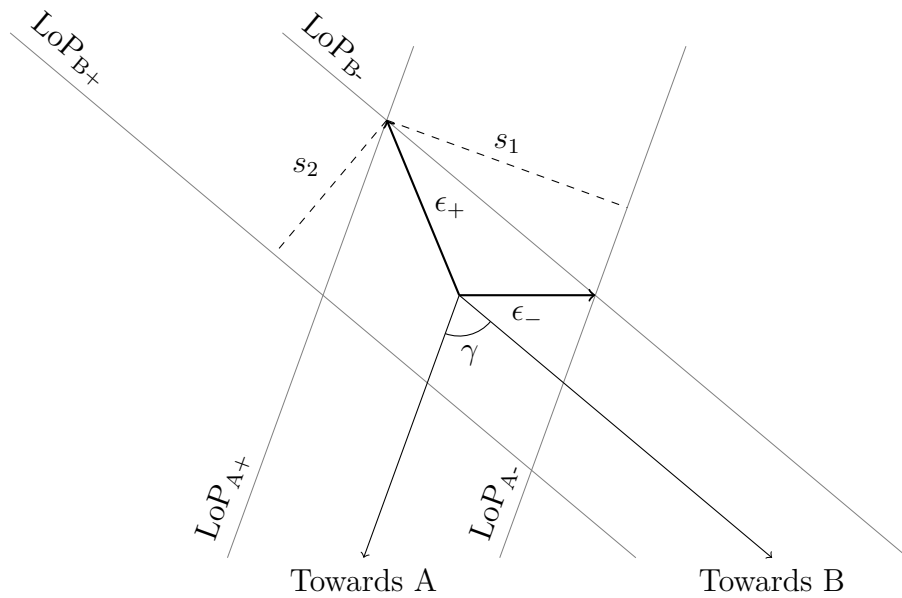
FIGURE 2.9: The detailed geometry at the transmitter's location.

Assuming the error in the positive and negative direction is equal, $\Delta_{\text{A+}} = \Delta_{\text{A-}} = \Delta_{\text{A}}$ and $\Delta_{\text{B+}} = \Delta_{\text{B-}} = \Delta_{\text{B}}$, yields $s_1 = 2\Delta_{\text{A}}$ and $s_2 = 2\Delta_{\text{B}}$. The magnitude of ϵ_+ and ϵ_- are found using simple trigonometry and are identical to (2.39) save for an interchange of signs.

$$\epsilon_+ = \frac{\Delta_A}{\sin\gamma}\sqrt{1 + \left(\frac{\Delta_B}{\Delta_A}\right)^2 + \frac{2\Delta_B}{\Delta_A}\cos\gamma} \tag{2.45}$$

$$\epsilon_- = \frac{\Delta_A}{\sin\gamma}\sqrt{1 + \left(\frac{\Delta_B}{\Delta_A}\right)^2 - \frac{2\Delta_B}{\Delta_A}\cos\gamma} \tag{2.46}$$

As can be seen from Figure 2.9, $\epsilon_+ > \epsilon_-$ for acute angles γ, and vice versa when γ is obtuse. This allows for a simplification:

$$
\begin{aligned}
\epsilon &= \begin{cases} \epsilon_+ & 0 < \gamma < 90° \\ \epsilon_- & 90° \leq \gamma < 180° \end{cases} \\
&= \frac{\Delta_A}{\sin\gamma}\sqrt{1 + \left(\frac{\Delta_B}{\Delta_A}\right)^2 + \frac{2\Delta_B}{\Delta_A}|\cos\gamma|} \qquad 0 < \gamma < 180° \qquad (2.47)
\end{aligned}
$$

Because Δ_A, Δ_B are dependent on the distances to the respective base stations further simplifications (as were done for the circular trilateration case in section 2.4.1.2) cannot be made.

It is apparent from equation (2.47) that the GDoP is minimized for $\gamma = 90°$ where the error will be: $\epsilon_{\min} = \sqrt{\Delta_A^2 + \Delta_B^2}$ and grows towards infinity for $\gamma = 0°, 180°$, i.e. when the transmitter is in line with the two base stations.

2.4.3   The time-of-flight method

Another way of determining the distance between a transmitter and receiver is to measure the time it takes for a signal to propagate between them. Because the speed at which electromagnetic signals travel in air is near constant, the distance a signal has traveled equals the propagation time multiplied by the propagation speed c. Assuming the time is measured from when a signal is sent the from base station A, $t_{A,Tx}$ to when a reply from the transmitter at the unknown location is detected, $t_{A,Rx}$, the round trip *time of flight* (ToF) is given by:

$$
t_{rt} = t_{A,Rx} - t_{A,Tx} \tag{2.48}
$$

The range is then given by:
$$
R = \frac{ct_{rt}}{2} \tag{2.49}
$$

2.4.3.1   Measurement accuracy

If the measured ToF includes an error Δ_t, the estimated distance is given by:

$$
\hat{R} = \frac{c(t_{rt} + \Delta_t)}{2} = R + \frac{c\Delta_t}{2} \tag{2.50}
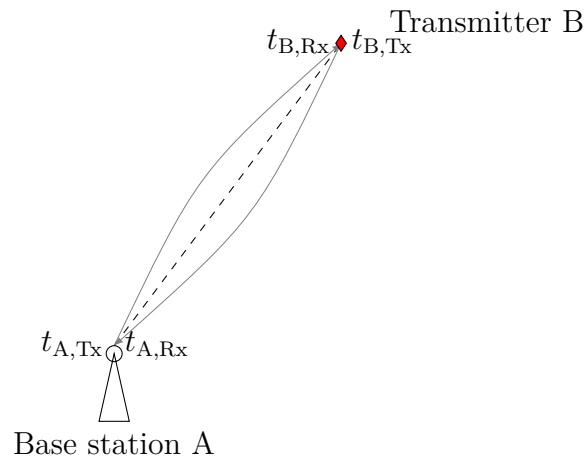$$

FIGURE 2.10: The time of flight, including the processing delay between the reception of the signal from the base station and the transmission of a reply.

This means that the estimation error, or residual, is not dependent of the range R, but only on the measurement error Δ_t.

Likely sources of error in the time measurement include:

- *Systemic errors*: delays internally in each device, e.g. the time from the timer is started until the signals start propagation away from the base station, the time from when the first signal is received at the other end until it is fully decoded and a reply starts propagating back towards the base station, and finally the delay between the signal arriving at the base station until the timer is stopped. These delays will be easily removed by calibration if they are constant.

- *Environmental errors*: Environmental issues may also affect the error; in a no line of sight (NLoS) situation the measured propagation time is that of the actual signal path, which may be longer than the distance between base station and transmitter.

2.4.3.2 Geometric dilution of precision

Because this is simply another way of doing circular trilateration, the geometric dilution of precision has the exact same form as described in Section 2.4.1.2.

2.4.4   The time-difference-of-arrival method

If the absolute propagation time cannot be determined, hyperbolic trilateration may
be used to locate the source, using the time difference of arrival (TDoA) for a pair
of base stations to calculate the propagation distance difference. If a signal from the
transmitter at unknown location (x, y) is received at times t_i and t_j at base stations
B_i and B_j, respectively, the TDoA can be defined by:

$$\tau_{i,j} = t_i - t_j \tag{2.51}$$

The corresponding difference of distance, assuming propagation at the speed of light,
c, will be $r_i - r_j = c\tau_{i,j}$, where r_i, r_j is the distance between the transmitter and
base stations i and j, respectively. Let the distance between base stations i and j
be denoted $d_{i,j} = \sqrt{(x_i - x_j)^2 + (y_i - y_j)^2}$.

Using a local coordinate system (x', y') oriented so that the base stations lie on the
x'-axis, symmetrically placed about the ordinate axis in points $(-c, 0)$ and $(c, 0)$
such that $2c = d_{i,j}$ as shown in Figure 2.11, the LoP for this base station pair given
by TDoA $\tau_{i,j}$ is defined in local coordinates by the *hyperbolic equation*:

$$\frac{x'^2}{a^2} - \frac{y'^2}{b^2} = 1 \tag{2.52}$$

Where $a = \frac{c\tau_{i,j}}{2}$, $c = \frac{d_{i,j}}{2}$ and $b = \sqrt{c^2 - a^2}$

An absolute distance difference results in a *pair* of hyperbolas, symmetric about
$y' = 0$, but in trilateration case that ambiguity may be eliminated because the
TDoA estimates are signed, i.e. it is known which base station picked up the signal
first. This is reflected in the sign of a, leading to the single hyperbola equation:

$$x' = a\sqrt{1 + \frac{y'^2}{b^2}} = \frac{c\tau_{i,j}}{2}\sqrt{1 + \frac{y'^2}{\frac{d_{i,j}^2 - c^2\tau_{i,j}^2}{4}}} \tag{2.53}$$

Now, the LoP can be plotted in *global* coordinates using the coordinate transforma-
tion in (2.54) where Δ_x, Δ_y is the translation and θ the counter-clockwise rotation
as illustrated in Figure 2.11.

$$\begin{bmatrix} x \\ y \end{bmatrix} = \begin{bmatrix} \cos\theta & -\sin\theta \\ \sin\theta & \cos\theta \end{bmatrix} \begin{bmatrix} x' \\ y' \end{bmatrix} + \begin{bmatrix} \Delta_x \\ \Delta_y \end{bmatrix} \tag{2.54}$$
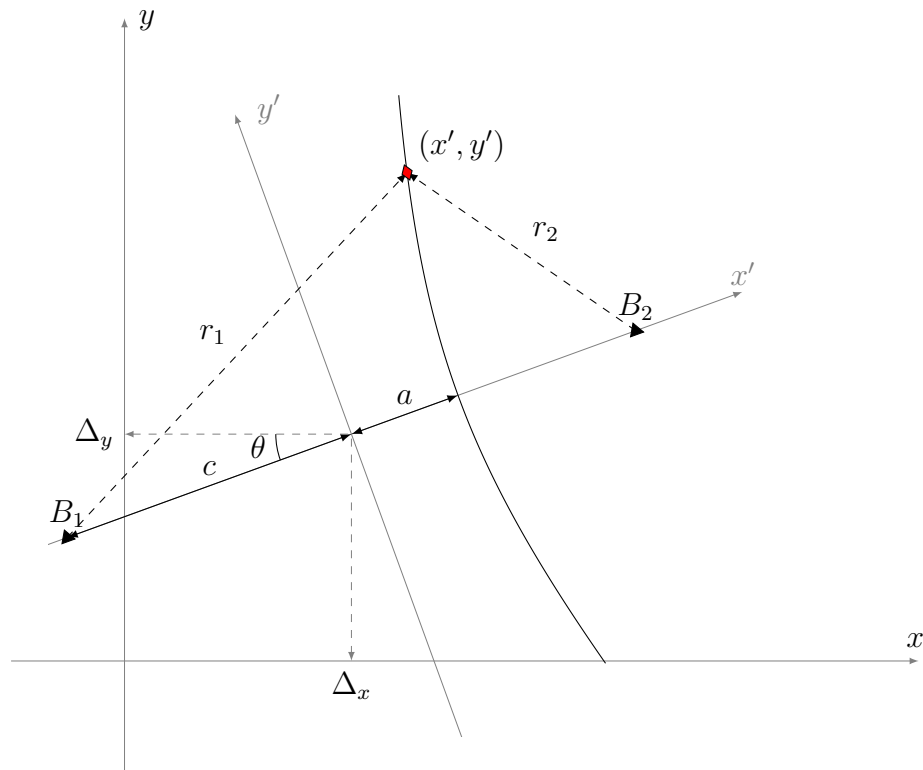
FIGURE 2.11: The local coordinate system (x', y') and the hyperbolic LoP given by the TDoA measurement τ_{ij}.

Computing the translation and rotation for each such local coordinate system as given by the base stations' fixed locations, the transformed hyperbolas may be plotted together in the global coordinate system to find the intersection locating the transmitter.

2.4.4.1 Measurement accuracy

Any delays in determining the exact time of arrival for each base station, as well as any asynchronicity between them will displace the LoP. If the total error in the TDoA is Δ_t, the entire hyperbola is transformed. The resulting shift will be smaller close to the baseline between the two base stations than at a distance, as shown in Figure 2.12.

Because of this complex relationship between the measurement accuracy and the geometry between the base stations and the transmitter, it does not make sense to discuss accuracy without introducing a third base station. Then, two LoPs may be constructed, leading to a position estimate. The accuracy of this estimate is detailed in the next section.
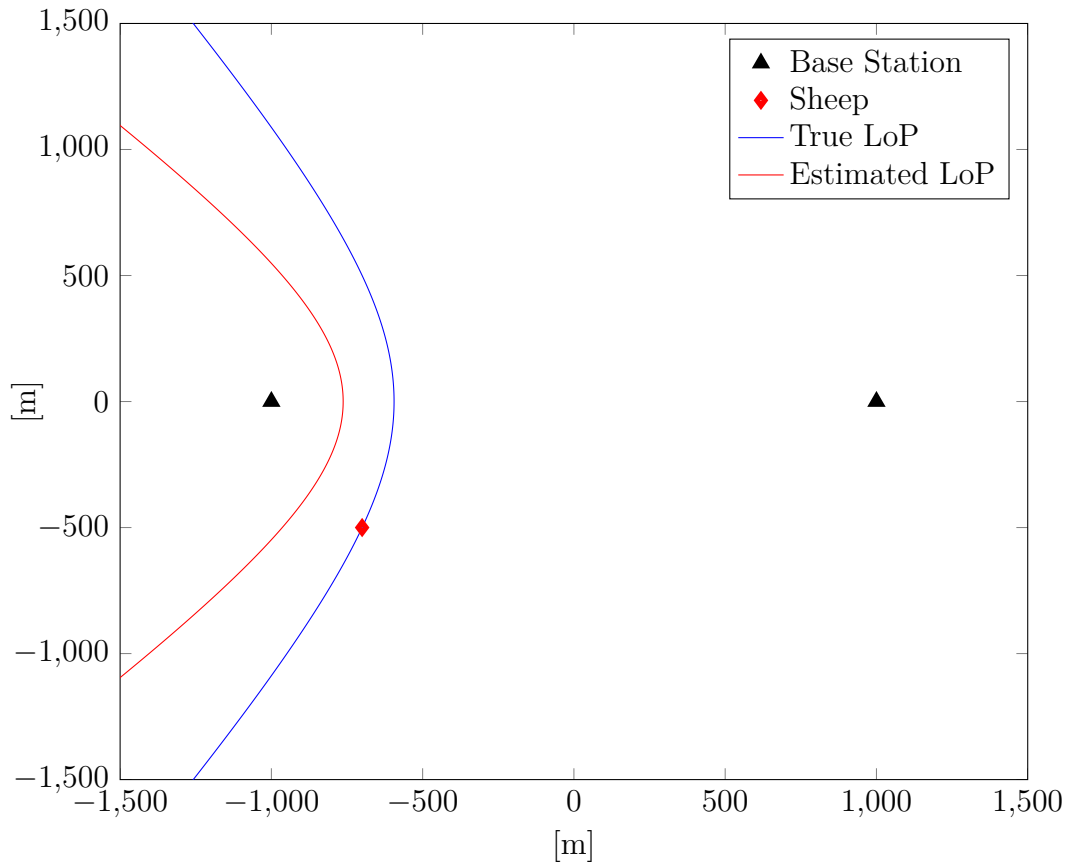
FIGURE 2.12: The error-free LoP (blue) intersects the sheep's position exactly. The red LoP is the result of a timing error $\sigma = 1\,\mu s$ at each base station.

2.4.4.2 Geometric dilution of precision

In hyperbolic trilateration systems as well as the circular ones, the geometry between base stations and the transmitter plays a role in the accuracy of the calculated position. Three base stations are needed to provide the minimum of two unique LoPs required to solve for the unknown position. This means there are now two aspect angles involved, as shown in Figure 2.13.

In [16], an expression is given for the mean squared positioning error. The derivation is quite involved, so only the final result is given here:

$$\overline{R^2} = \frac{\sigma^2}{4\sin^2\gamma}\left(\frac{1}{\sin^2\frac{\alpha}{2}} + \frac{1}{\sin^2\frac{\beta}{2}} + \frac{\cos\gamma}{\sin\frac{\alpha}{2}\sin\frac{\beta}{2}}\right) \tag{2.55}$$

FIGURE 2.13: The aspect angles determining the GDoP in hyperbolic trilateration.

Where:

$\overline{R^2}$ [m] : Mean squared positioning error

σ^2 [m] : Mean squared error in TDoA estimates

α : The angle between bearings towards base stations 1 and 2

β : The angle between bearings towards base stations 1 and 3

$\gamma = \dfrac{\alpha + \beta}{2}$

The error is minimized for $\alpha = \beta = 120°$, in which case it amounts to:

$$\overline{R^2_{\min}} = \frac{2\sigma^2}{3}, \quad \alpha = \beta = 120° \tag{2.56}$$

Dividing (2.55) by $\overline{R^2_{\min}}$ leads to a normalized expression for the error, i.e. it shows the factor by which the error grows depending on the geometry between the base stations and the transmitter. Figure 2.14 shows a contour plot of this GDoP factor.

The square root of the normalized error gives

$$G = \frac{\overline{R^2}}{R_{\min}^2} = \frac{1}{2\sin\gamma}\sqrt{\frac{3}{2}\left(\frac{1}{\sin^2\frac{\alpha}{2}} + \frac{1}{\sin^2\frac{\beta}{2}} + \frac{\cos\gamma}{\sin\frac{\alpha}{2}\sin\frac{\beta}{2}}\right)} \qquad (2.57)$$

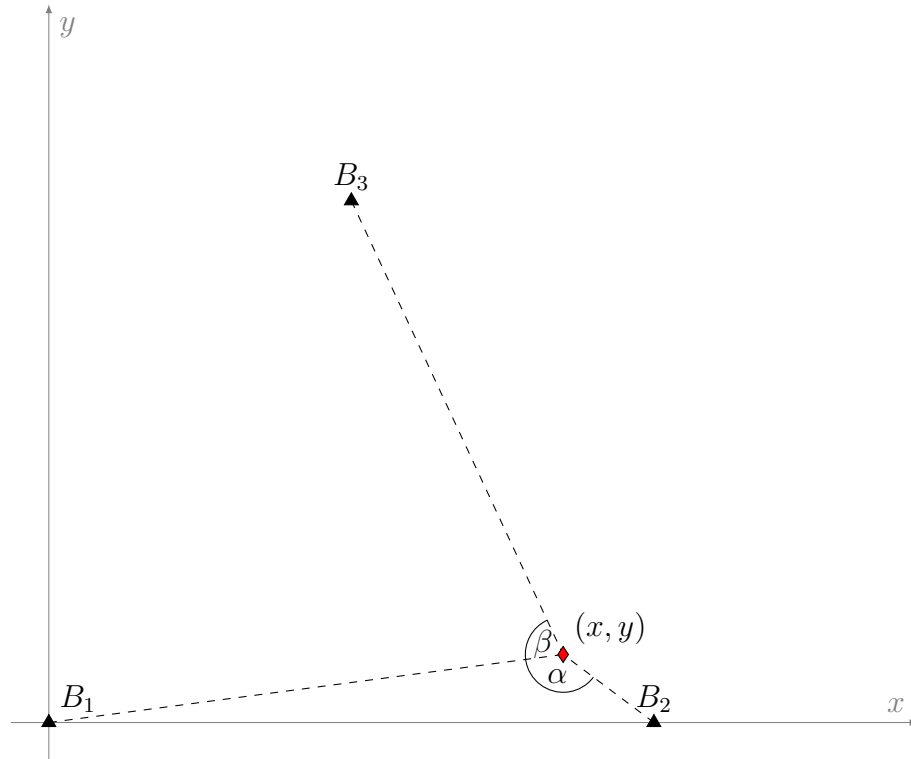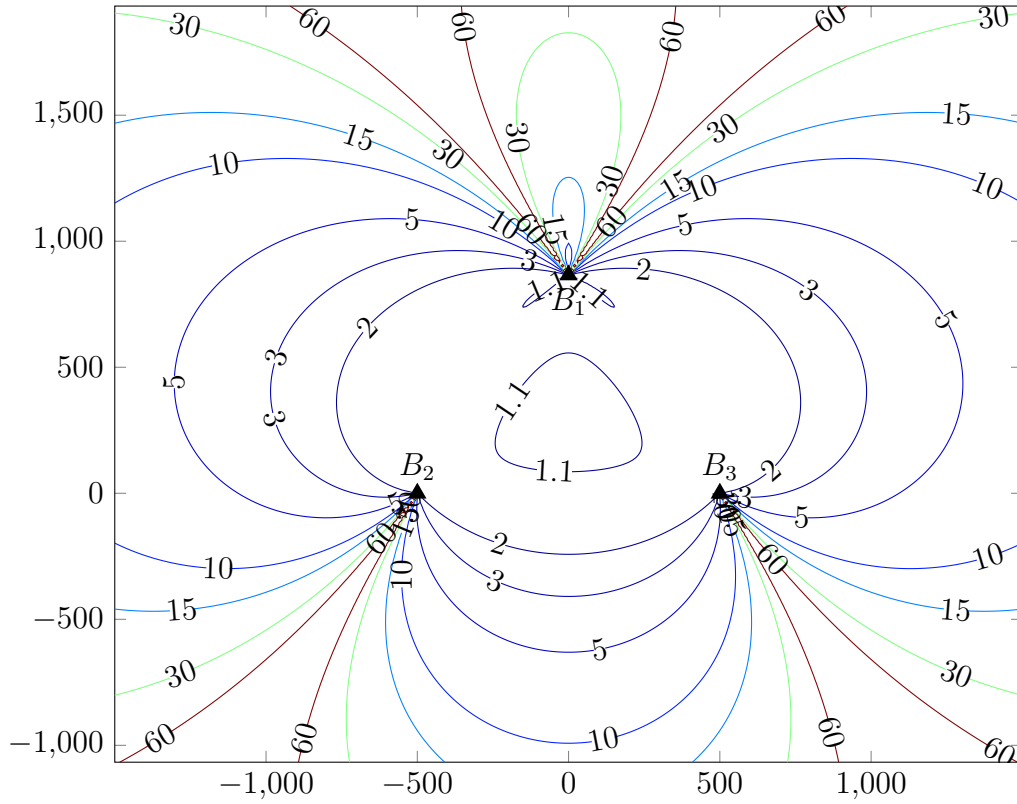FIGURE 2.14: Contour plot showing the factor by which the positioning error is worsened due to its relative placement to the base stations.

Chapter 3

Methodology

This chapter will discuss the different methods for performing the radio location using the CC1120 transceiver, and the expected accuracy for each method. All measurements involving the CC1120 are done using the TrxEB rev. 1.7.0 evaluation board from Texas Instruments, along with antennae from the evaluation kit for the CC1120 transceiver series. The evaluation module has an on-board oscillator with frequency $f_{\mathrm{XOSC}} = 32\,\mathrm{MHz}$.

3.1 RSSI estimation

The CC1120 evaluates received signal strength (RSSI) as part of its *automatic gain control* (AGC) circuit. The RSSI estimate is the output of a moving-average filter defined by:

$$RSSI_k = \frac{1}{N}\left(P_k + P_{k-1} + \cdots + P_{k-N+1}\right) \tag{3.1}$$

Where $RSSI_k$ denotes the current RSSI estimate, and $P_k, P_{k-1}, \ldots, P_{k-N+1}$ are the received power for the N most recent samples that are used as input to the filter. On the CC1120, the value for N can be set to 2,3,5 or 9 by configuring the `AGC_CFG0.RSSI_VALID_CNT` register.[13, Chap. 6.9]

The current value for the RSSI estimate is a 12-bit two's complement number stored in the registers `RSSI1.RSSI_11_4` (8 MSB) and `RSSI0.RSSI_3_0` (4LSB). The resolution is $0.0625\,\mathrm{dB}$ resulting in a dynamic range of $-128\,\mathrm{dBm}$ to $127.9375\,\mathrm{dBm}$.
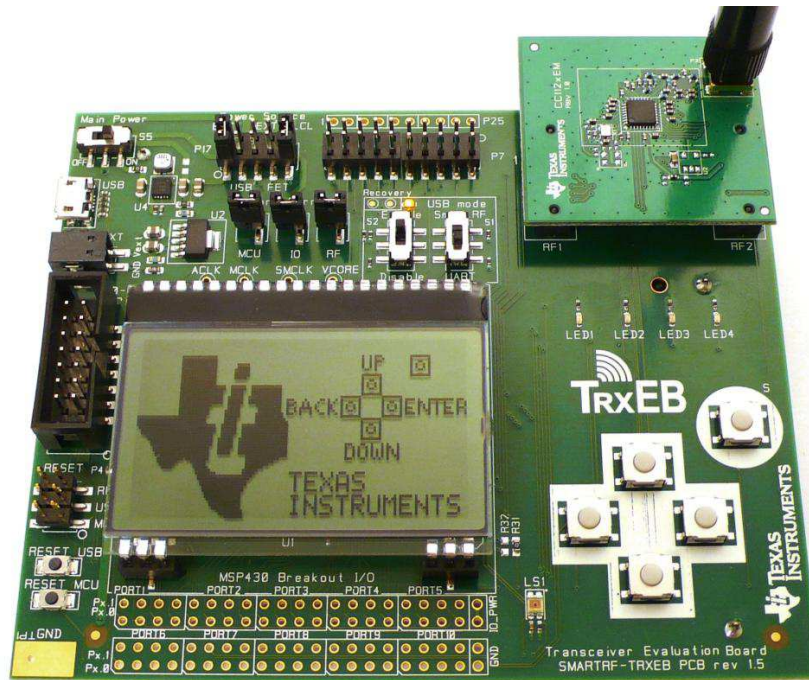
FIGURE 3.1: The TrxEB evaluation board fitted with a CC1120 evaluation module and antenna.

Because the signal power received at the terminals of the LNA is a function of antenna-, impedance- and polarization losses as well as the actual electromagnetic field strength at the base station, a calibration is necessary if the values stored in the CC1120's register are reflect the actual reception conditions. This calibration can be done by inputting a signal of known power to the receiver, reading the RSSI estimate from the register, and calculating the difference. This difference is stored in the `AGC_GAIN_ADJUST.GAIN_ADJUSTMENT` register, and is used to shift all future RSSI estimates accordingly.

Using the CC1120's built-in RSSI estimation for trilateration requires no additional circuitry; the individual RSSI estimates can be stored and tagged with an approximate time of reception as well as a transmitter ID corresponding to where it came from. Because the system is intended to transfer some data to a backbone, the RSSI estimates will just be a part of this information, and the actual trilateration will take place in a designated master control station, which can be one of the base stations or a separate computer communicating with the base stations.

3.2 TDoA estimation

A crucial part of any TDoA location algorithm is the accuracy of the time-difference measurements. The ability of the base station to determine the exact time of arrival of any incoming signal and time stamp it is the most critical part in providing good position estimates. Each time-stamp can then be compared to that of other base stations, and serve as basis for constructing the hyperbolas.

In this section, the CC1120 transceiver's ability to determine the time of difference of arrival will be examined by looking at different output signal that the chip can be configured to output upon reception of data.

The TDoA location method will use a GPS-disciplined oscillator (GPSDO) to provide an accurate time and frequency standard in the base stations. Using this solution, the delay between the clocks in any two base stations should be less than $10\,\text{ns}$. See Section 3.3 for details around this technology. With an accurate time reference, a binary counter clocked by the oscillator will provide the numerical value for the reception time of a signal. Comparing these values from a pair of base stations will give a TDoA value. If the GPSDO has a frequency of 100 MHz, an integer number of cycles given by the counter corresponds to a time-scale resolution of:

$$\frac{1}{100\,\text{MHz}} = 10\,\text{ns} \tag{3.2}$$

The block diagram in Figure 3.2 shows the main components required in the base stations to compute TDoA measurements.

3.2.1 The sync word.

The CC1120 radio is equipped with four general purpose input/output (GPIO) pins, GPIO3-0. These pins may serve a host of different functions, controlled individually via setting the register `IOCFGx.GPIOx` on the transceiver's main register, where x is 0, 1, 2 or 3.[1]

The `PKT_SYNC_RXTX` signal is one of these signals. Each packet transmitted by the CC1120 contains an 11-32 bit long synchronization word transmitted directly after the variable length preamble, but before the payload. The `PKT_SYNC_RXTX`

---

[1]The CC1120 User's Guide provides a detailed list of all registers and their settings. It may be downloaded at: `http://www.ti.com/lit/ug/swru295e/swru295e.pdf`.
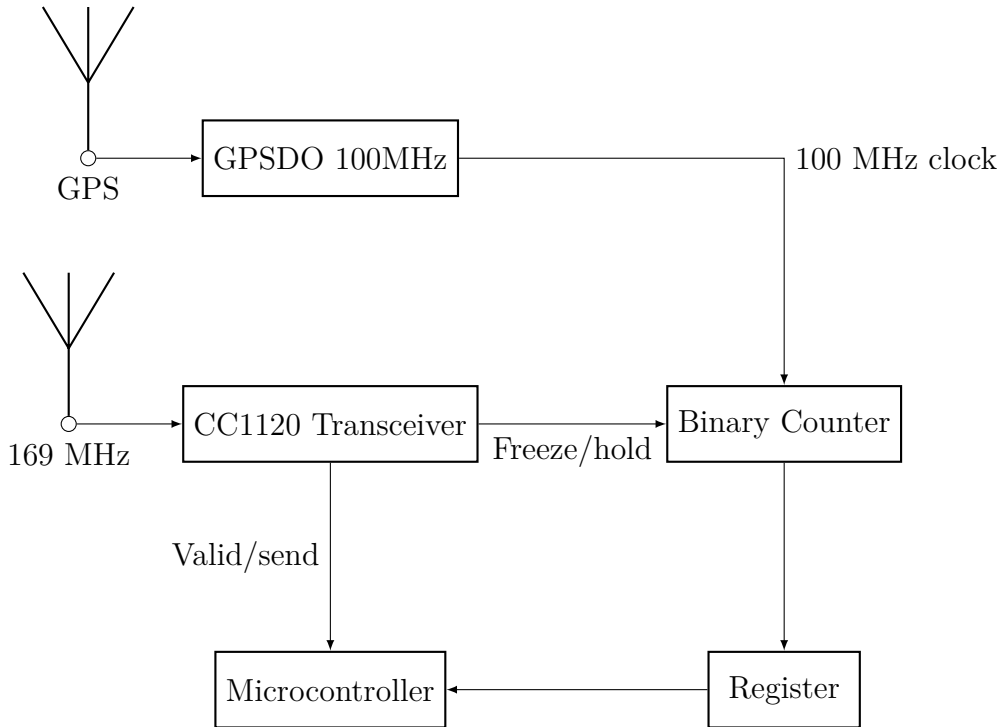
FIGURE 3.2: A proposed structure for the base station in a hyperbolic trilatera-
tion system, using a GPS-disciplined oscillator as time standard.

signal is asserted upon detection of the sync word and de-asserted at the end of
the packet. This signal may be outputted on any GPIO pin by setting the pin's
corresponding register value `IOCFGx.GPIOx_CFG` = 6 (0x06), where the 0x prefix
indicates a hexadecimal value.[13, Chap. 3.4]

To determine if this signal is asserted consistently and with a fixed delay with respect
to the reception of the signal, the signal was measured simultaneously from two
receivers. A single antenna was connected to both receivers using a power divider to
ensure that both receivers obtained the exact same signal. The GPIO2 pin on each of
the receivers was configured to output the `PKT_SYNC_RXTX` signal, and connected to
separate channels on an oscilloscope. The transmitter was configured to continuously
send identical packets at a fixed interval, so that the oscilloscope could trigger at
that interval to compare the two outputs. The set-up is illustrated in Figure 3.3.
The measurements were carried out for various transmission parameters. Due to
the antennae and evaluation modules from the evaluation kit being designed for
a 868 MHz carrier, that is what is being used in these experiments rather than
169 MHz. This should not affect the timing capabilities of the CC1120 as the onboard
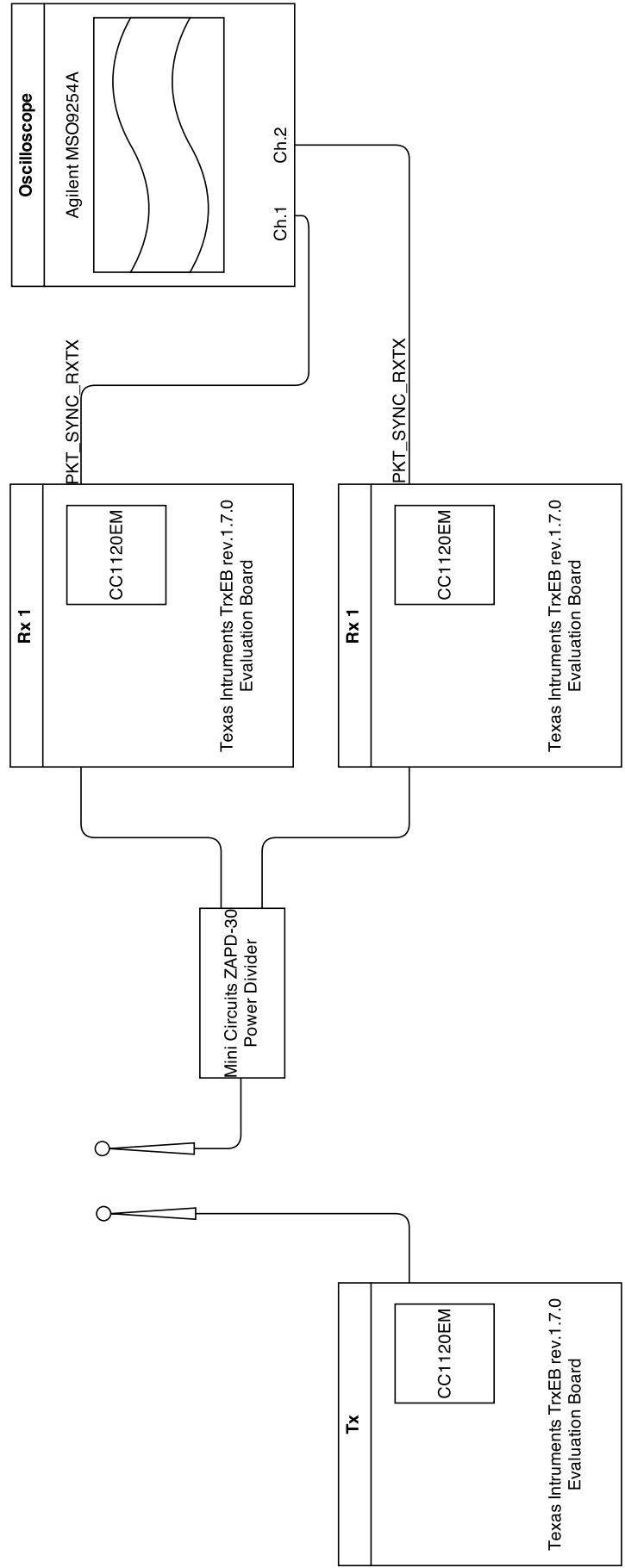oscillator has the same frequency regardless of the carrier wave.

FIGURE 3.3: The setup used for measuring the timing of the PKT_SYNC_RXTX signal.

3.2.1.1   Performance using 1.2 ksps symbol rate

The transmitter was set to use 868 MHz carrier frequency, 50 kHz bandwidth, 1.2 ksps symbol rate and 2-FSK modulation, i.e. binary frequency shift keying. With these transmission parameters, the result is that the `PKT_SYNC_RXTX` signals are is not outputted synchronously from the receivers. As shown by Figure 3.4, there is a delay of more than 100 μs between the two for this particular packet. Neither is the delay between the two signals constant; the measurements showed that it changes with every packet received. This might be due to the receivers entering a sleep state at the end of each received packet, shutting down its on-board oscillator. The on-board oscillators are therefore not synchronised when the transmitters power back up. The variable delay was measured for a number of packets and its statistics are given in table 3.1. It is apparent that signals are never further apart than about 200 μs. This indicates that the signal is determined at a rate of about $\frac{1}{200\,\mu s} =$ 5000 Hz. This rate is about 4 times the symbol rate of 1200 symbols per second.

(A) At 50 ms/div.   (B) At 50 μs/div.

FIGURE 3.4: The `PKT_SYNC_RXTX` signal from both receivers @ 1.2 ksps, showing a delay. Screenshot from Agilent MSO9254A Oscilloscope.

3.2.1.2   Performance using 25 ksps symbol rate

The same test was performed again using a higher symbol rate to see if it would affect the outcome. Under a 50 kHz bandwidth constraint, the maximum symbol rate for 2-FSK (binary frequency-shift-keying) is 25 ksps. As shown in Figure 3.5, the delay is significantly smaller, around 10 μs for this particular packet. This corresponds to a frequency of $\frac{1}{10\,\mu s} = 100$ kHz, again 4 times the symbol rate.
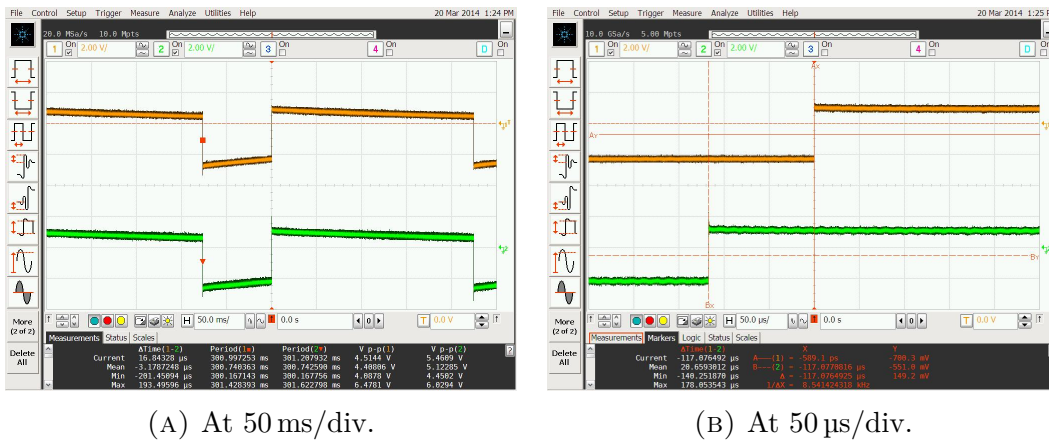
(A) At 20 ms/div.

(B) At 5 µs/div.
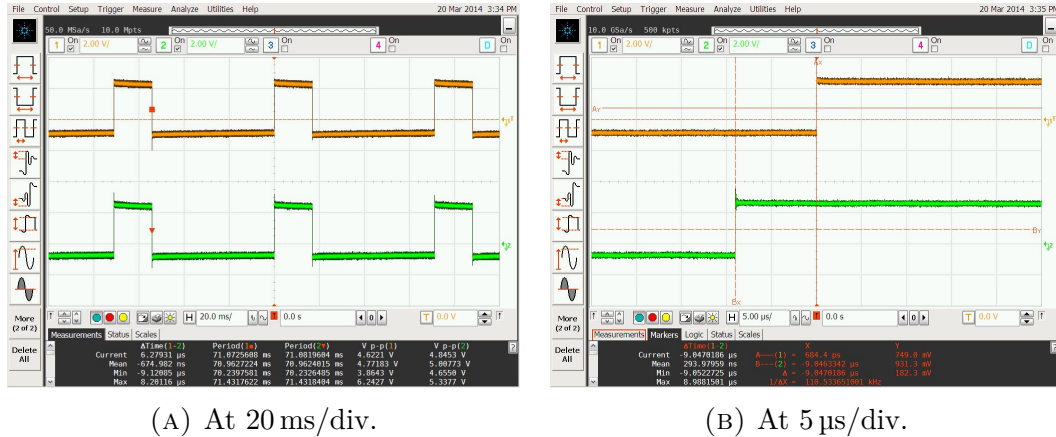
FIGURE 3.5: The `PKT_SYNC_RXTX` signal from both receivers @ 25 ksps, showing a delay. Screenshot from Agilent MSO9254A Oscilloscope.

Symbol rate [ksps]	1.2	25
No. of measurements [µs]	1078	4113
Max [µs]	199.25	9.63
Min [µs]	-208.85	-10.30
Mean [µs]	-1.39	-0.314
Std. deviation [µs]	85.51	4.11

TABLE 3.1: Statistics for the delay between the `PKT_SYNC_RXTX` signal at two receivers for different symbol rates.

3.2.2 The preamble detector

The CC1120 uses a preamble to help synchronise timing between transmitter and receiver. The preamble is a bit stream of alternating 0's, 00's, 1's and 11's of programmable minimum length between 0.5 and 30 bytes. The preamble allows the receiver to extract the bit rate from the incoming symbols and prepare to detect a sync word designating the beginning of the packet's payload.

The detection is done using a 8 bit wide correlation filter to judge the incoming preamble.[13, Chap. 6.8] A preamble quality estimator is output from the filter, stored and continuously updated in the register `PQT_SYNC_ERR.PQT_ERROR`. When this estimator is smaller than a preprogrammed threshold, the preamble is determined to be valid and the bit synchronisation should be good enough to start detecting the sync word. When the threshold is passed, the CC1120 can be set to output the signal `PQT_REACHED` on one of its GPIO pins by setting `IOCFGx.GPIOx_CFG = 11 (0x0B)`

(A) 1.2 ksps, 100 µs/div.   (B) 25 ksps, 10 µs/div.
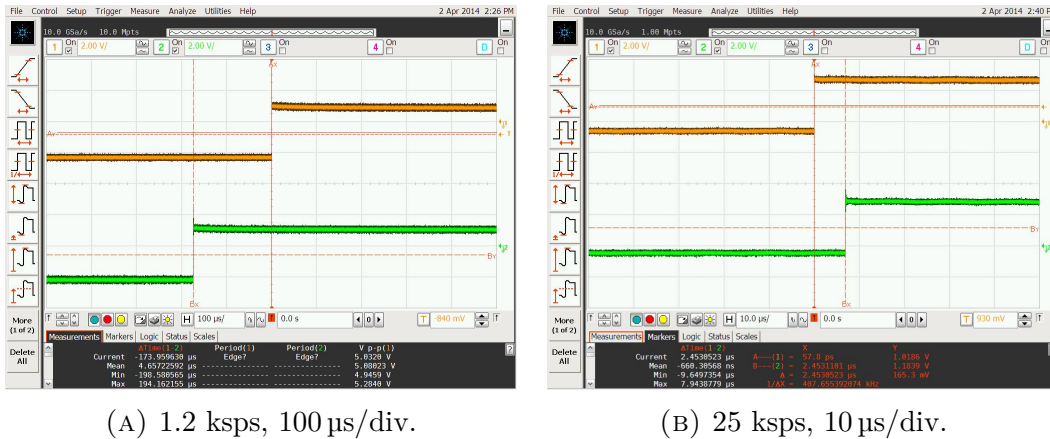
FIGURE 3.6: The `PQT_REACHED` signal from both receivers at two different symbol rates, showing a delay. Screenshot from Agilent MSO9254A Oscilloscope.

Symbol rate [ksps]	1.2	25
No. of measurements	1137	1319
Max [µs]	204.0	9.2
Min [µs]	-198.6	-9.7
Mean [µs]	1.6	-0.5
Std. deviation [µs]	84.3	4.1

TABLE 3.2: Statistics for the delay between the `PQT_REACHED` at two receivers for different symbol rates.

The synchronisity between the two receivers was measured in the same way as shown in Figure 3.3. The transmission parameters were the same as those used to measure the `PKT_SYNC_RXTX` signal. Figure 3.6 shows an example of the oscilloscope output for one packet. Table 3.2 lists the statistics for the measurements.

These results are similar to what was found for the `PKT_SYNC_RXTX` signal in Section 3.2.1, so even though the preamble detection happens earlier in the signal chain than the sync word detection there was no gain in timing accuracy from using the `PQT_REACHED` signal.

3.2.3 Other signal options: PLL lock and Carrier Sense

Two more of the CC1120's internal signals were analysed in the same manner as described in Section 3.2.1, without showing any improvement in terms of accuracy.

- *The* `LOCK` *signal* : This signal is set high as soon as the CC1120's phase-locked-loop (PLL) achieves a lock (phase-synchronicity) with the carrier wave. It can

Symbol rate [ksps]	25
No. of measurements	1362
Max [µs]	44.5
Min [µs]	-45.6
Mean [µs]	-0.5
Std. deviation [µs]	15.1

TABLE 3.3: Statistics for the delay between the `PKT_SYNC_RXTX` at 25 ksps at the two receivers with clock extraction enabled.

be output to either `GPIO1` or `GPIO0` by setting the register `IOCFGx.GPIOx_CFG` = 35 (`0x23`) .

- *The* `CARRIER_SENSE` *signal*: This signal is set high whenever the CC1120 detects a carrier wave with power above a pre-set threshold. This signal should only be interpreted when the signal `CARRIER_SENSE_VALID` is high. These signals may be output to either of the four `GPIO` pins by setting the register `IOCFGx.GPIOx_CFG` = 17 (`0x11`) for `CARRIER_SENSE` or 16 (`0x10`) for `CARRIER_SENSE_VALID`.

Another possible improvement is to force the CC1120 to do a clock recovery based on the incoming symbols. This i possible when the expected symbol rate is known.[13, chap. 6.6] Setting the register `TOC_CFG` = 78 (`0x4E`) ensures that the clock extraction from the incoming signal is as accurate as possible. When this setting was in effect, the pair of CC1120's showed less accurate performance than before. As shown in Table 3.3 the delay between the two at 25 ksps symbol rate was in the range $(-45\,\mu s, +45\,\mu s)$, meaning the signal is clocked out at a frequency of $\frac{1}{45\,\mu s} \approx 22.2\,kHz$, more or less the same as the symbol rate. This deterioration is most likely due to the added complexity in the decoding stage that causes a variable delay.

3.2.4 Direct bit stream logging

To get better time accuracy than what can be achieved by reading status signals from the GPIO ouputs, it is necessary to use outputs closer to the amplifier in the signal chain, see Figure 3.7. The CC1120 has the option to output a bit stream directly from the AD converter. The signal's in-phase (I) and quadrature (Q) components are tapped directly after the intermediate frequency (IF) ADCs and output serially using low-voltage differential signalling (LVDS). The signal sampling in the ADCs

is performed at half the rate of the onboard oscillator, $f_{\text{ADC}} = \frac{f_{\text{XOSC}}}{2} = 16\,\text{MHz}$. The CC1120 has single ADCs, i.e. 1 bit/sample, and the serial format is [I 1 Q 0] so 4 bits are transmitted for each sample, leading to a LVDS symbol rate of $f_{\text{LVDS}} = 4 \times 16\,\text{MHz} = 64\,\text{MHz}$.

This rate is too high for most common microcontrollers to be able to capture the signal successfully, including the MSP430[2] which can be found on the evaluation board used for the CC1120.

One option is to use an FPGA to decode the bit stream at the receiver and buffer it for a certain amount of time whenever a packet is received. Then, the sequence can be time-stamped and transmitted to a master control station, e.g. a base station designated as such. Using cross-correlation, the delay between the different signal sequences with respect to the time stamps can be found, ideally down to a resolution of one sample period, $\frac{1}{16\,\text{MHz}} = 62.5\,\text{ns}$, assuming perfectly synchronised time-stamps. Using GPS receivers at the base station, a 1 pulse-per-second signal synchronized to within $10\,\text{ns}$ of GPS time can be used for this purpose.

3.3   Accuracy of the GPS timing signal

In any hyperbolic positioning system the base stations must have clocks with a high degree of synchronicity as to be able to produce accurate TDoA measurements. Traditionally, the *network time protocol* (NTP) has been used in packet based distributed networks to achieve accuracy between nodes to within "a few microseconds".[17]

If a higher level of synchronisation is necessary, e.g. in TDMA telecommunication systems, the only solution up until recently has been to include one or more Rubidium frequency standards in the network, providing a frequency standard that is accurate to within 5×10^{-12}, 5 *parts per trillion*, but at prices of US$ 1000 the Rubidium standard is an unreasonable cost for this system, because each client will need multiple base stations.

---

[2]Texas Instruments MSP430F5438A, supports AD-conversion up to $32\,\text{Msamples/s}$, $\frac{1}{4}$ of the minimum sampling rate needed to decode the LVDS signal. See `http://www.ti.com/product/msp430f5438a`
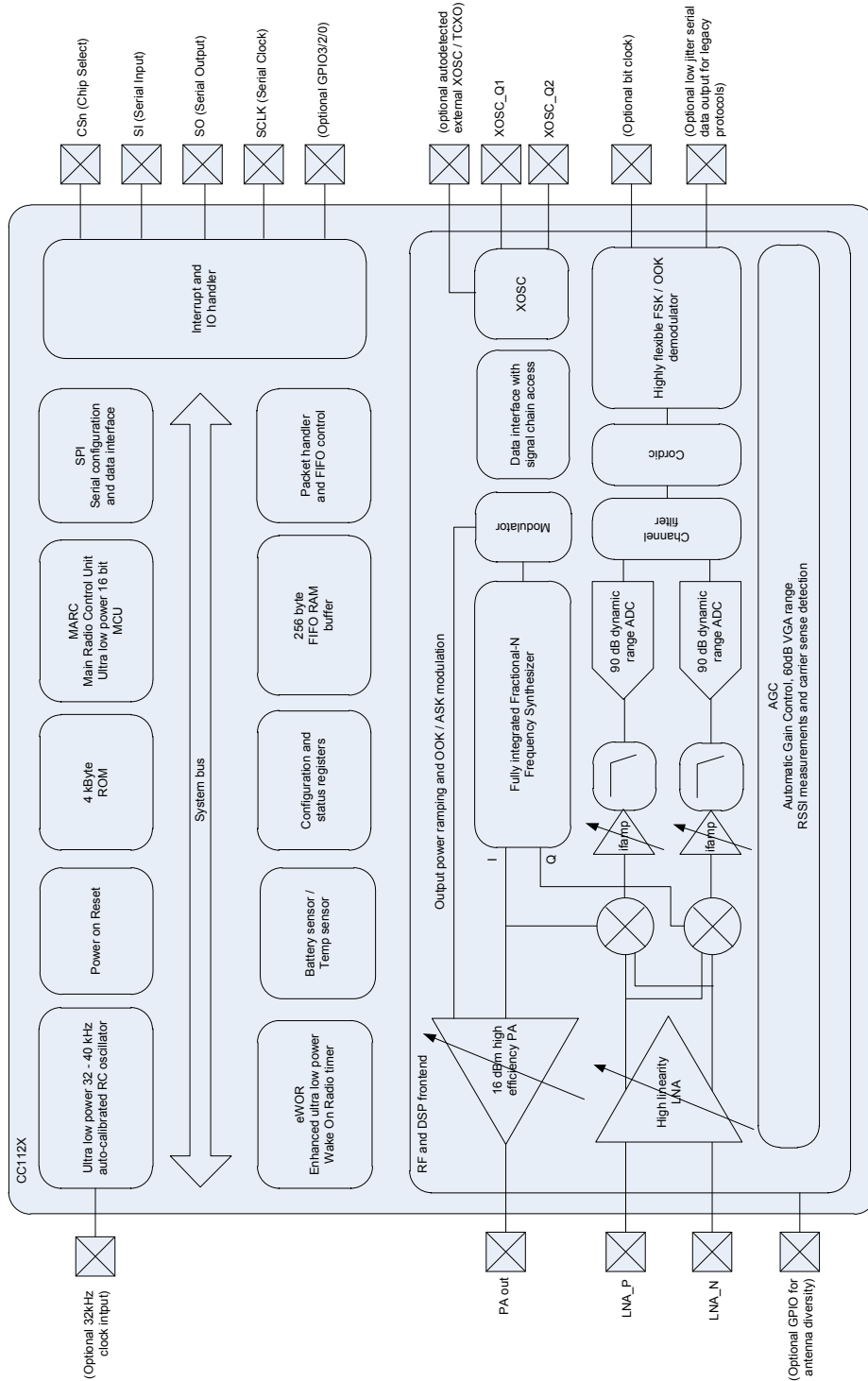
FIGURE 3.7: A simplified block diagram showing the different stages in the CC1120 transceiver.

A relatively new, viable alternative is to use a *GPS-disciplined oscillator* (GPSDO), which combines the excellent short term stability of a oven-controlled crystal oscillator (OCXO) with the long-term stability of a 1-pulse-per-second (1PPS) signal generated by a GPS receiver. This results in a frequency standard that is accurate enough to act in some applications as an affordable alternative to the Caesium standards from which the very definition of a second is derived. This is because the GPS satellites themselves carry multiple Caesium or Rubidium standards on board, whose stability is critical to the operation of the system.

In effect, GPS receivers costing less than US\$ 100 are capable of delivering a 1PPS signal that is within 10 ns of *universal coordinated time* (UTC),[3] the current global time standard. Disciplining a OCXO with this signal results in a frequency standard with a typical accuracy of 3×10^{-10}, or 0.03 Hz at 100 MHz.[4]

3.4   Proposed base station structure

In the finished system, the base stations will need some hardware in addition to the CC1120. One possible solution design is to use an FPGA to read ADC data directly from the CC1120 as discussed in Section 3.2.4. If the data is continuously buffered whenever a packet is detected, the 1 pulse-per-second signal from the GPS receiver can be used to time-stamp the data accurately. The bit stream will be stored upon reception of a packet, and sent to the master control station. There, it can be compared to bit streams from other base stations, and using cross-correlation the TDoA value can be determined. The accuracy of this estimate will depend on the length of the bitstream and the sample rate of the ADC.

---

[3]Such as the Quectel L70, `http://www.quectel.com/UploadFile/Product/Quectel_L70_GPS_Specification_V2.1.pdf`

[4]An example is the Symmetricom GPS-2600, `http://www.microsemi.com/document-portal/doc_download/133407-gps-2600-and-gps-2650`

Chapter 4

An RSSI Experiment

This chapter will present an experiment that was performed to investigate the feasibility of using the built-in signal strength indicator (RSSI) on the CC1120 transceiver to estimate propagation distances in the base station network and ultimately determine a transmitter's position in the plane based on these estimates.

After presenting the experiment setup, a method for calibration of the propagation model will be detailed, followed by the resulting estimates in range (one-dimensional estimates) and position (two-dimensional).

4.1 Calibration of the propagation model

To find out whether the CC1120's RSSI measurements may be used for location in reality, an experiment was carried out using a pair of CC1120 evaluation modules mounted to "TrxEB" evaluation boards from Texas Instruments. All measurements were done in the park area surrounding the Kristiansten Fort in Trondheim. Three points were selected as "base station" points and 15 additional points as measuring points. Each point's position was marked on the ground and its GPS coordinates recorded using a smartphone. Figure 4.1 shows the position of these points; base stations are marked with triangles and measuring points with squares. The lettering/numbering will be used throughout this chapter to refer to specific base station or measure point locations.[1]

---

[1]Zohar Bar-Yehuda's MATLAB script `plot_google_map` was used to create MATLAB plots with background maps from google. See `http://www.mathworks.com/matlabcentral/fileexchange/27627-plot-google-map`
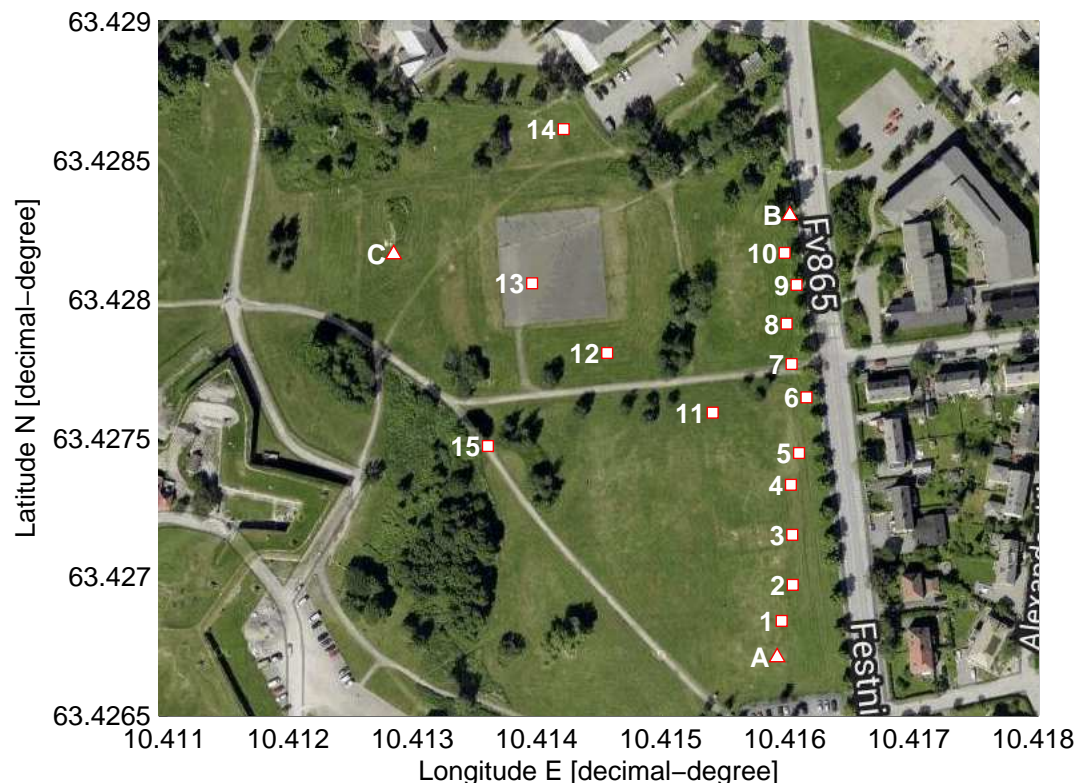
FIGURE 4.1: The true position of base stations and measuring points for the experiment. Map and satellite image overlay courtesy of Google Maps.

At the base station, the evaluation board was connected to a laptop to log incoming packets along with time of reception and RSSI level for each packet. The board was positioned on an inverted plastic bucket raising it 40 cm above ground. The other evaluation board, the transmitter, was battery powered and moved successively through each measuring point. For each point it was positioned according to the marked position on the ground, and set to transmit packets continuously using the "EasyLink" sample software bundled with the TrxEB (rev 1.7.0).[18]

Once in position and transmitting, the receiver at the base station was switched on and set to receive 10 consecutive packets. The packets are logged on the laptop and saved to a file containing the time of reception, packet sequence number, payload and RSSI value at the start of the packet. The payload was set to be 28 bytes of randomized data.

This was repeated for all 15 measuring points with the receiver in three different "base station" positions. The logged RSSI values were read from the transceiver's register `RSSI1.RSSI_11_4` which contains the 8 most significant bits of the most

recent RSSI estimate. This results in a 1 dBm precision in the stored value. As shown in Figure 4.2, the RSSI measurements were fluctuating between each packet, at times quite heavily. The figure shows the RSSI estimates at base station A for measuring points 1 through 10.
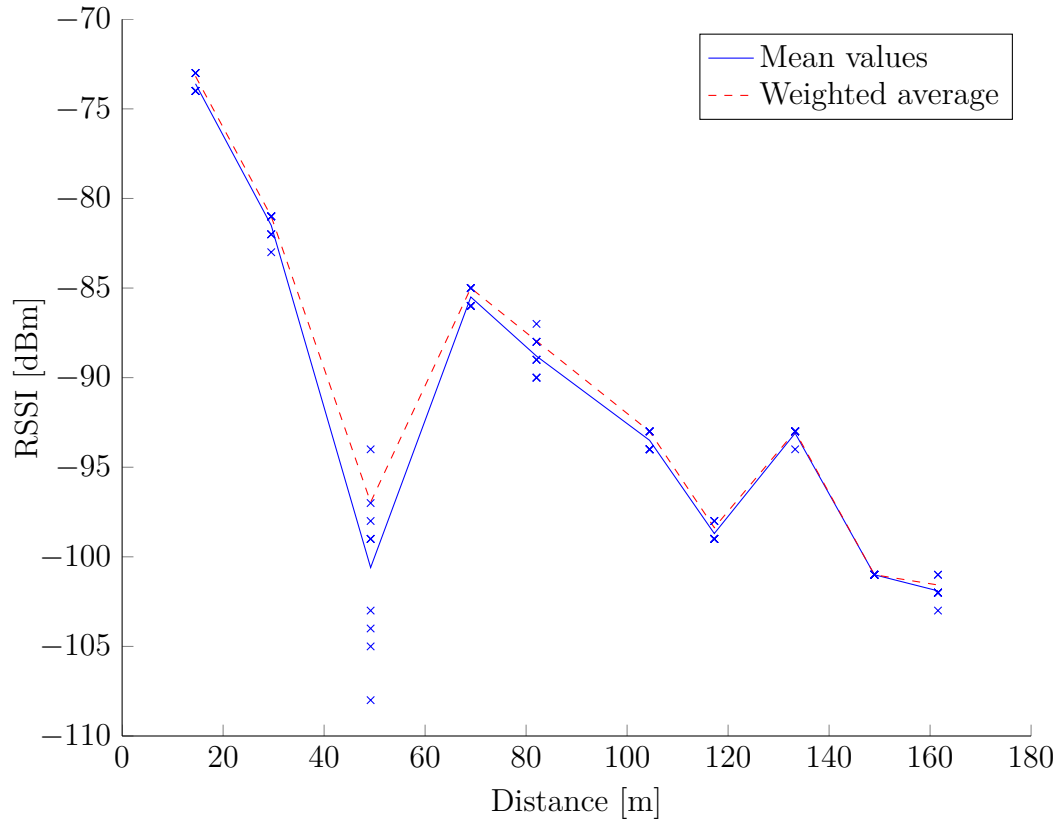
FIGURE 4.2: The RSSI measurements at base station A for measuring point 1 through 10 and their deviations. The red dashed line show how a weighted average can reduce the impact of weak outlier values.

As discussed in Chapter 2.4.1, the received signal power may experience sudden drops due to channel fading. Figure 4.2 shows that the RSSI for the third measurement point ranges from -94 dBm to -108 dBm. This means that the lowest measured signal strength is 14 dB lower than the strongest measurement for that point, a reduction by more than 95%.

One way of dealing with adverse multi-path effects as this one is to utilize some form of diversity. *Spatial* diversity means having multiple antennas at the receiver or transmitter separated by at least a half wave length, ensuring that if one antenna is in a deep fade zone due to interference, at least one other will be unaffected. This was not attempted in the experiment for practical reasons.

Another form of diversity is *temporal* diversity, which in the case of this experiment amounts to transmitting the same packet several times, in the hope that negative circumstances affecting one measurement will not last long enough to ruin the other nine. In this experiment, the packets were transmitted at an interval of 300 ms, meaning the last RSSI estimate was made 3 seconds after the first. This amounts to a form of repetition coding, see [15, chap. 3].

To mitigate fading errors, the five lowest values for the RSSI estimate were discarded. The average of the remaining five values was computed and used for the distance estimation. The red dashed line in Figure 4.2 represents these weighted averages. All averaging is done on values in watts, and then converted back to dBm. Not doing this will lead to artificially low average values because of the logarithmic nature of the dBm unit.

With reference in Friis' free space transmission equation (2.30), the relationship between distance and measured RSSI may be simplified as shown in [19, chap.4] to the following:

$$RSSI = -10n\log(R) + A \Leftrightarrow R = 10^{\frac{A-RSSI}{10n}} \tag{4.1}$$

Where the different quantities are:

$$n \text{ [unitless]} : \qquad \text{path loss exponent}$$
$$R \text{ [m]} : \qquad \text{distance between transmitter and receiver}$$
$$A \text{ [dBm]} : \qquad \text{RSSI measured at } R = 1 \text{ m}$$

Recalling Friis' equation, rearranging terms of (2.30) and isolating for $P_{r,\text{dBm}}$ yields:

$$P_{r,\text{dBm}} = 20\log\left(\frac{\lambda}{4\pi}\right) - 20\log(R) + P_{t,\text{dBm}} + G_{t,\text{dB}} + G_{r,\text{dB}} \tag{4.2}$$

Comparing this with (4.1), the following relationship emerges:

$$n = 2$$
$$A = 20\log\left(\frac{\lambda}{4\pi}\right) + P_{t,\text{dBm}} + G_{t,\text{dB}} + G_{r,\text{dB}} \tag{4.3}$$

Measuring A in the environment that is used for testing eliminates the need to determine transmitter and receiver gain, as well as transmitter power. It also eliminates the need to calibrate the RSSI offset in the receiver, see Section 3.1. The path loss

exponent n may then be determined by isolating for it in equation (4.1) and solving it based on RSSI measurements done at known distances.

4.1.1 The 1-metre reference value A

The value for A is dependent on the settings and hardware that is being used, including carrier frequency, transmitter power, antenna directionality and polarization, amplifier gain and impedance mismatch losses. To measure A, the transmitter was placed at a distance of 1 metre from the base station. Ideally, the antennas should be completely isotropic, but to ensure omni-directionality the reference value was measured several times rotating the base station through a full revolution.

The resulting average value for the one-metre reference is $A = -45\,\text{dBm}$. Note that because no calibration of the CC1120 was done beforehand, this value does not represent the actual received power, but this offset is cancelled out in the $A - RSSI$ term in (4.1).

4.1.2 The path loss exponent n

The exponent n describes how quickly the received signal power at the base station decreases as distance to the transmitter increases. For free space propagation, $n = 2$ as shown by Friis' transmission equation (2.30). In complex environments such as forests, this value is expected to be quite a bit higher as a result of propagation losses and signal interference; experiments in [20] show values ranging from 1.4 indoors to 5.5 in a dense forest. Figure 4.3 shows RSSI as given by the formula in equation (4.1) for a few different values of n.

To determine a value for n for this experiment, an approach was taken using linear regression (linear least-squares). As shown in Figure 4.3, there is no linear relationship between the distance and RSSI because of the logarithmic function. Still, if $\log(R)$ is used as a variable in place of R, equation (4.1) becomes a linear function with intercept A and slope $-10n$. Using all 15 measurements for all 3 base stations in the experiment gives $n = 45$ data points to perform the regression on. Let $x_i, y_i \quad (i = 1, 2, ..., n)$ denote distance between transmitter and receiver and the measured RSSI, respectively, for data point i. *Ordinary least squares linear regression* may then be performed using the method described in [21, Chap. 11] by the
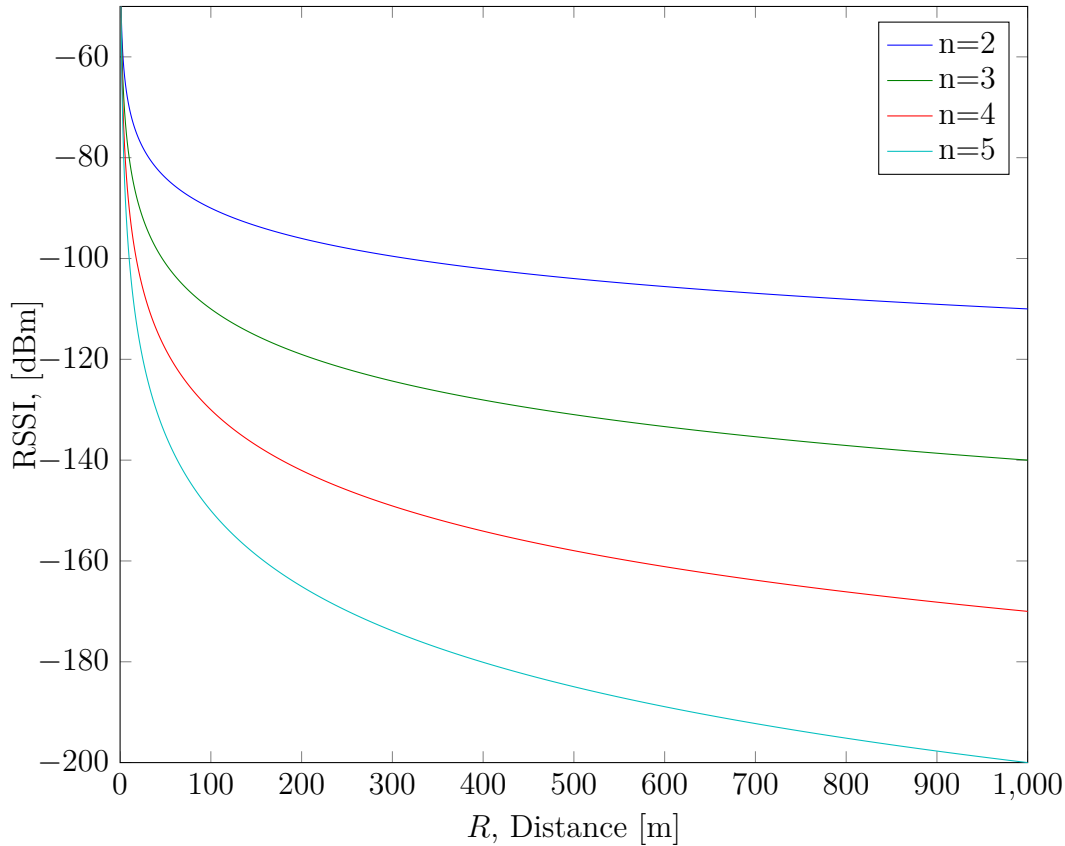
FIGURE 4.3: Expected RSSI vs. distance for 4 different values of n.

formula:

$$\beta = \frac{\sum_{i=1}^{n}(x_i - \bar{x})(y_i - \bar{y})}{\sum_{i=1}^{n}(x_i - \bar{x})^2} \tag{4.4}$$

$$\alpha = \bar{y} - \beta\bar{x} \tag{4.5}$$

Where α, β are the intercept and slope of the linear approximation, and $\bar{x}, \bar{y}$ are the average distance and RSSI value, respectively. Figure 4.4 shows the data points along with the linear approximation. The calculated slope of the line is $\beta \approx -25.9$, corresponding to a path loss exponent of $n = 2.59$.

The use of ordinary least-squares approximation in the estimation of n may prove too sensitive to outlier samples in data sets with extreme outlier values. A more robust approach is to use the *Theil-Sen estimator* as defined by Henri Theil in [22].

Using an open-source MATLAB script[2] to calculate an alternative slope by the Theil-Sen estimator resulted in a value of $n = 2.53$, which is the one used throughout the

---

[2]Credit goes to A. Tilgenkamp for the `Theil_Sen_Regress` function, which may be found at
`http://www.mathworks.com/matlabcentral/fileexchange/34308-theil-sen-estimator`

remainder of this experiment.
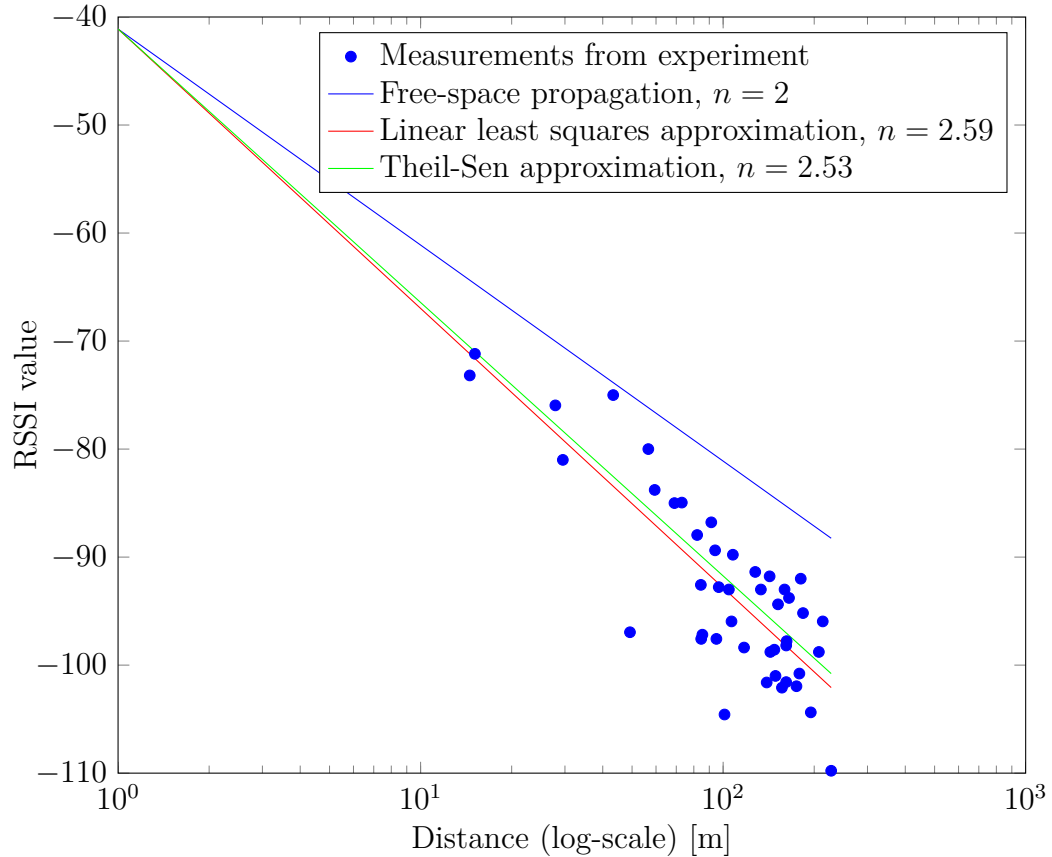
FIGURE 4.4: All the RSSI measurement vs the distance from their respective base stations.

4.2 Map projection

To calculate the true distances between base stations and measuring points based on the latitude/longitude coordinates obtained by GPS, the *inverse haversine formula* is used. It is a formula for calculating the great-circle distance d between two points on a sphere given by:

$$d = 2r \arcsin\left(\sqrt{\sin^2\left(\frac{\phi_2 - \phi_1}{2}\right) + \cos(\phi_1)\cos(\phi_2)\sin^2\left(\frac{\lambda_2 - \lambda_1}{2}\right)}\right) \qquad (4.6)$$

Where:

ϕ_1, ϕ_2 [rad] :   Latitudes of point 1 and 2.

λ_1, λ_2 [rad] :   Longitudes of point 1 and 2.

d [m] :   Great-circle distance on the sphere between point 1 and 2.

r [m] :   Radius of the sphere.

These distance calculations are based on a spherical earth model with a radius of $r = 6371.009$ km, which is the mean radius based on the oblate spheroid defined under the WGS84 geodetic system, the reference frame used in the GPS system.[3] Because the earth's radius of curvature is about 1% greater at the poles than at the equator, the great-circle distance as given by (4.6) is only accurate to within 0.5% when using the mean radius.

To project the spherical coordinates of the base stations and measuring points into a Cartesian coordinate system, the origin was placed at 63.4265°N, 10.4120°E, an arbitrary point selected in the south west corner of the Kristiansten park where the experiment was performed. The coordinate system was oriented so that the x-axis (abscissa) lies along the east/west direction and the y-axis (ordinate) along the north/south direction. The longitudes were then mapped to x-values, and the latitudes to y-values using the inverse haversine formula (4.6).

This very simple projection is a flattening of the surface of the sphere, and leads to a slight overestimation of distances along any direction that is non-parallel to either axis. Calculating the great-circle distance $d(\phi_1, \lambda_1, \phi_2, \lambda_2)$ between two points in the general area where the experiment took place, for example $p_1 = 63.40\,°\text{N}, 10.40\,°\text{E}$ and $p_2 = 63.41\,°\text{N}, 10.41\,°\text{E}$ using (4.6) results in:

$$d(63.40, 10.40, 63.41, 10.41) \approx 1218.29\,\text{m} \tag{4.7}$$

The Euclidean distance between the same two points in the (x, y) coordinate system is given by:

$$\sqrt{d(63.40, 10.40, 63.40, 10.41)^2 + d(63.40, 10.40, 63.41, 10.40)^2} \approx 1218.32\,\text{m} \tag{4.8}$$

---

[3]The WGS84 standard is defined by the *World Geodetic Standard and Geomatics Focus Group* (WGSG-FG) at the National Geospatial Intelligence Agency, on behalf of the U.S. Department of Defense. The standard's identifier is MIL-STD-2401 and may be downloaded at `https://nsgreg.nga.mil/doc/view?i=2058`

The difference between the two is $3\,\mathrm{cm}$, which is deemed negligible for all purposes of this experiment.

4.3   One-dimensional results

In terms of pure ranging, i.e. estimation of the distance between the base station and the transmitter, the second variant of equation (4.1) is used. The values for A and n are found through measurements and least squares approximation as detailed in Sections 4.1.1 and 4.1.2. Figures 4.5 through 4.7 show the estimated range alongside the true range for all three base stations.

Figure 4.8 shows the distribution of the error made by all of the distance estimates. The majority of errors are negative, i.e. the estimated distance is shorter than the true distance. This means the received signal is stronger than what was to be expected for that distance using the current propagation model. Possible reasons for this include reflections causing constructive interference, most likely ground reflections, the estimated path loss exponent n being too large, or the 1-metre reference value A being too small.

The figure shows that almost 50% of the errors are in the range -40 m to 0 m.

FIGURE 4.5: The estimated distance and the true distance from base station A
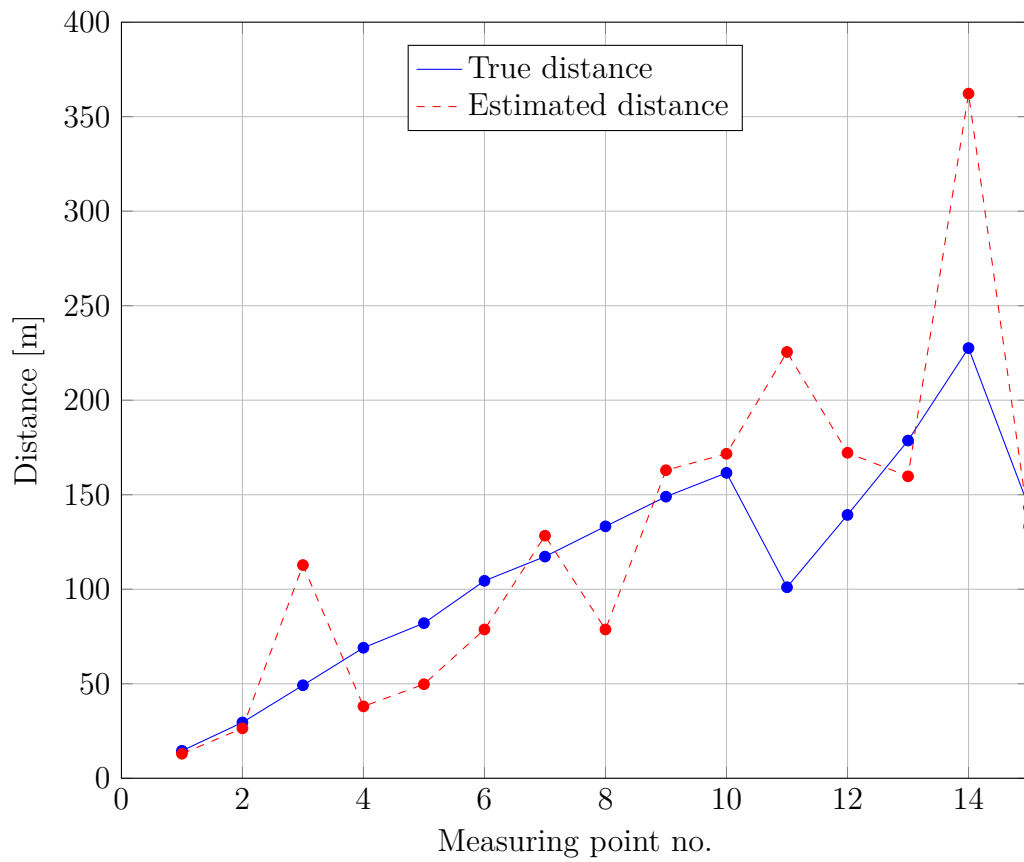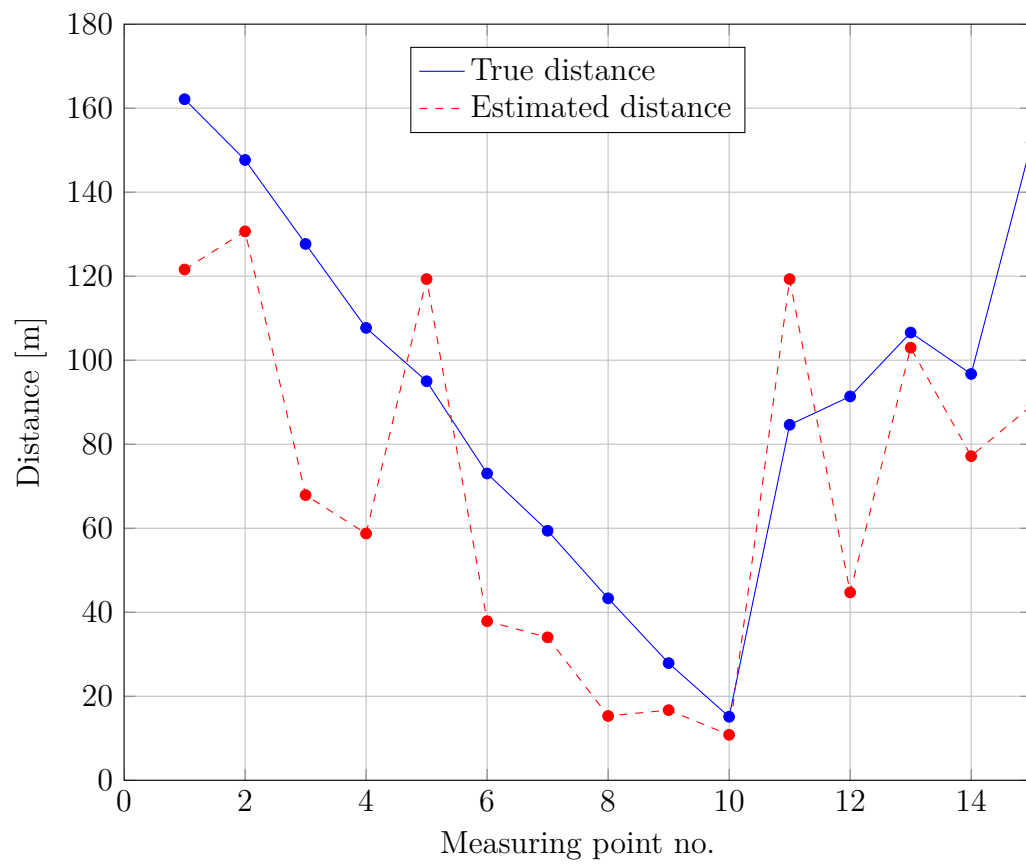to each measuring point.

FIGURE 4.6: The estimated distance and the true distance from base station B to each measuring point.
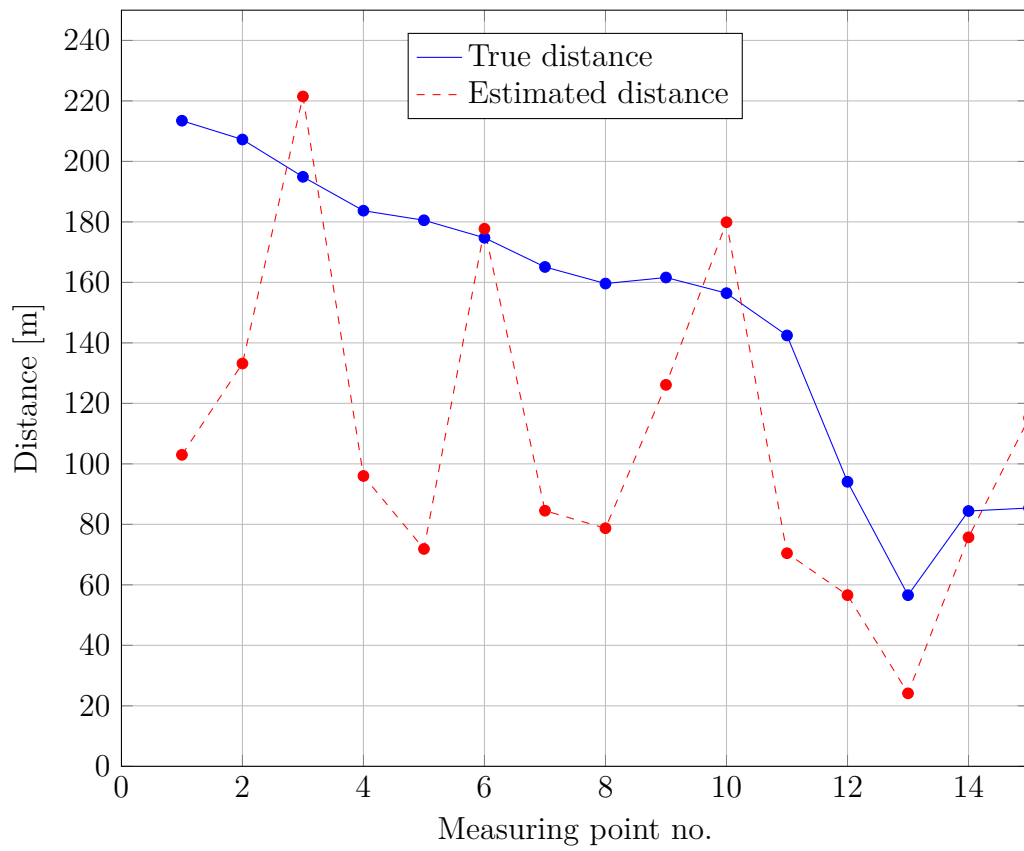
FIGURE 4.7: The estimated distance and the true distance from base station C
to each measuring point.
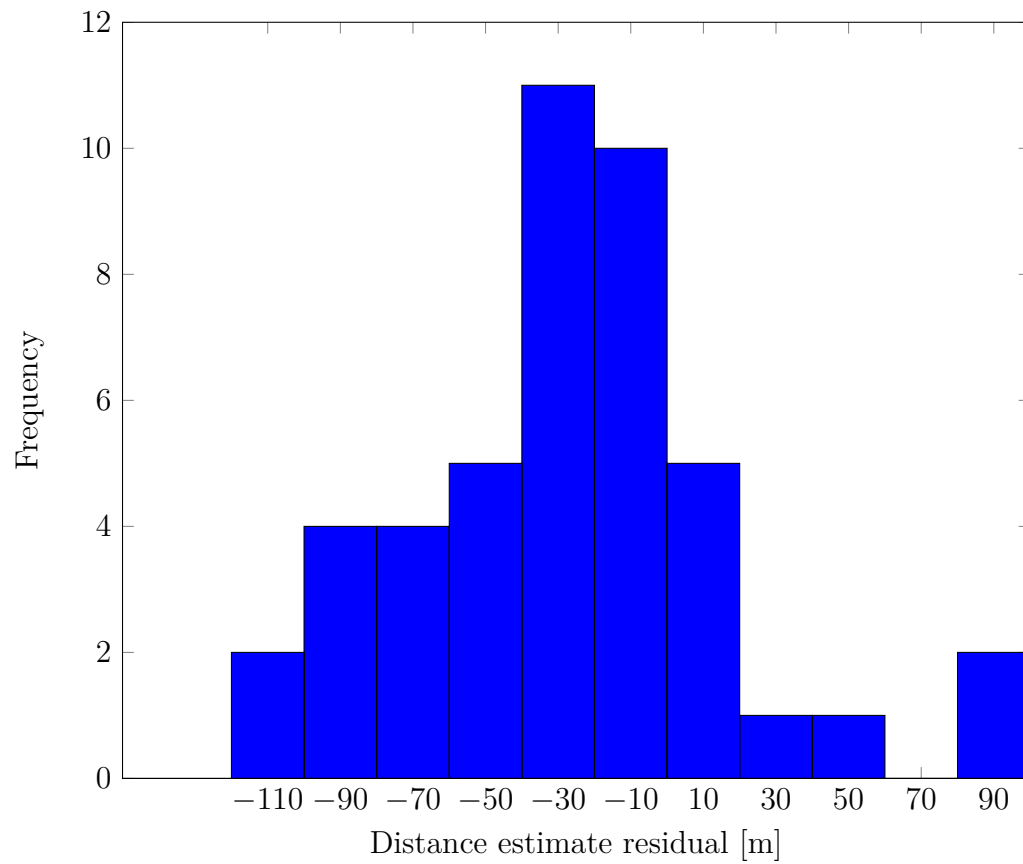
FIGURE 4.8: The difference between true distance and estimated distance for all 45 estimations.

4.4 Two-dimensional results

Using the distance estimates from the previous section, location can be performed using the trilateration techniques discussed in Section 2.4.1.2. When the range estimates are very accurate, the exact position can be found by using three base stations and solving the two resultant equations of (2.6). As shown in Figure 4.9 this is not always the case; the range estimates are far from accurate, and there is no single point of intersection of the LoPs. In effect the position that is found by solving the linearised equation system (2.6) contains an error. This error may be minimized by including estimates from more than three base stations. This turns (2.6) into an over-determined system, and an approximate solution may be found by applying a linear or non-linear least squares approximation technique, as described in section 2.2.2 and 2.2.3, respectively.

FIGURE 4.9: The base stations and their respective LoPs according to the estimated ranges for measuring point no. 2. Note that there is no clear point of intersection.

In this experiment, only three base stations were available at all times. That means that the linearised equation set (2.6) is fully determined, and a least squares position estimate may be calculated using (2.7).

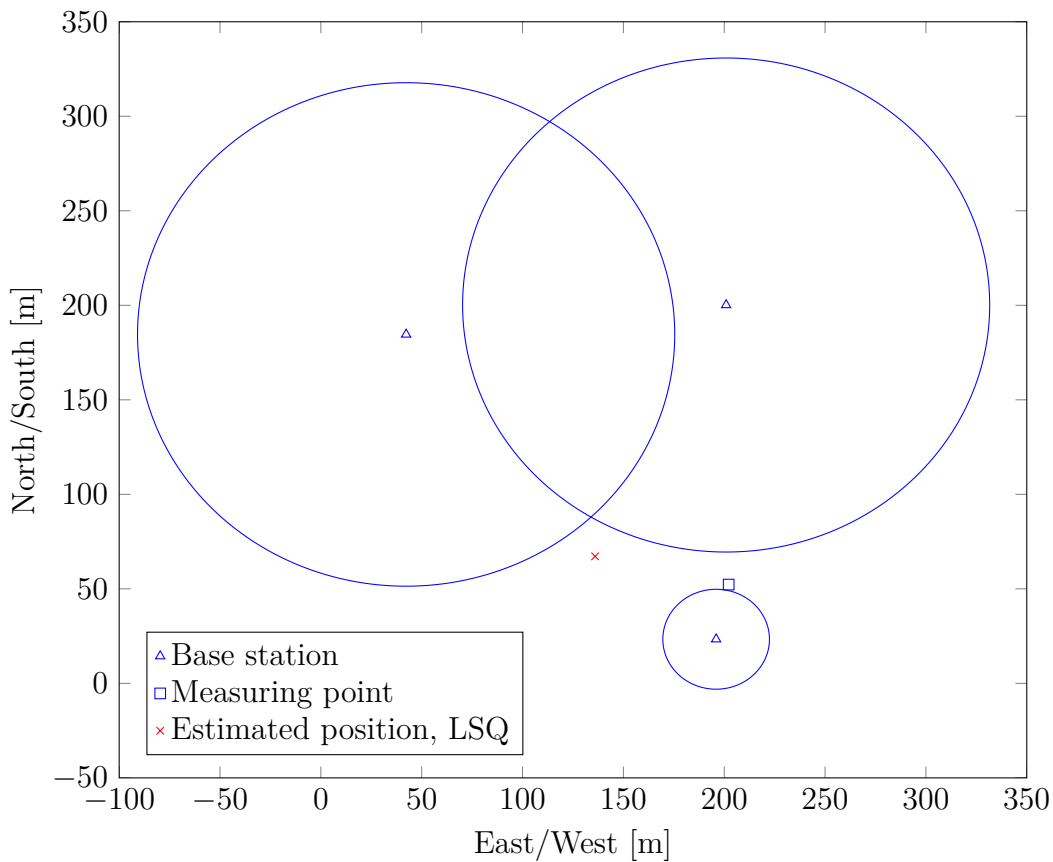Alternatively, using the non-linear distance equations directly, a least squares solution can be found using the iterative Gauss-Newton algorithm described in section 2.2.3. The linear least squares approximation will be used as the initial position for the algorithm. Then the algorithm is set run until the step length falls below $0.1\,\mathrm{m}$ or a maximum of 10 steps is reached, whichever comes first.

Solving for x and y based on the range estimates presented in section 4.3 yields the position estimates shown in Figure 4.10. The errors in the position estimates are shown in Figure 4.11. As shown, in most cases the Gauss-Newton algorithm gives an estimate that is about the same as the direct solution of the linearised problem. For measuring point 14 the non-linear least squares (NLSQ) estimate is significantly more accurate, reducing the error from $235\,\mathrm{m}$ to $55\,\mathrm{m}$.

The improvement of the NLSQ estimates over the linearised solution is expected to increase when more than 3 base stations are included. Additionally, range estimates based on base stations far away may be given lower weight than the closer ones in the calculation.

Based on the discussion around the geometrical dilution of precision (GDoP) in Section 2.4.1.2, the position estimates that form an *aspect angle* of $90°$ with any two base stations are expected to be the most accurate. For the various measuring points in this assignment, points 4–7,14 and 15 are the ones closest to fulfilling this property. Conversely, points 1,10,11 and 13 have aspect angles that are more acute or obtuse than what is optimal. However, looking at the positioning errors in Figure 4.11, the error seems to be more prone by random variations than GDoP, most probably due to propagation effects.

The numerical values for the positions and their estimates, as well as the one-dimensional ranges and their estimates from the previous section may be found in Appendix A.
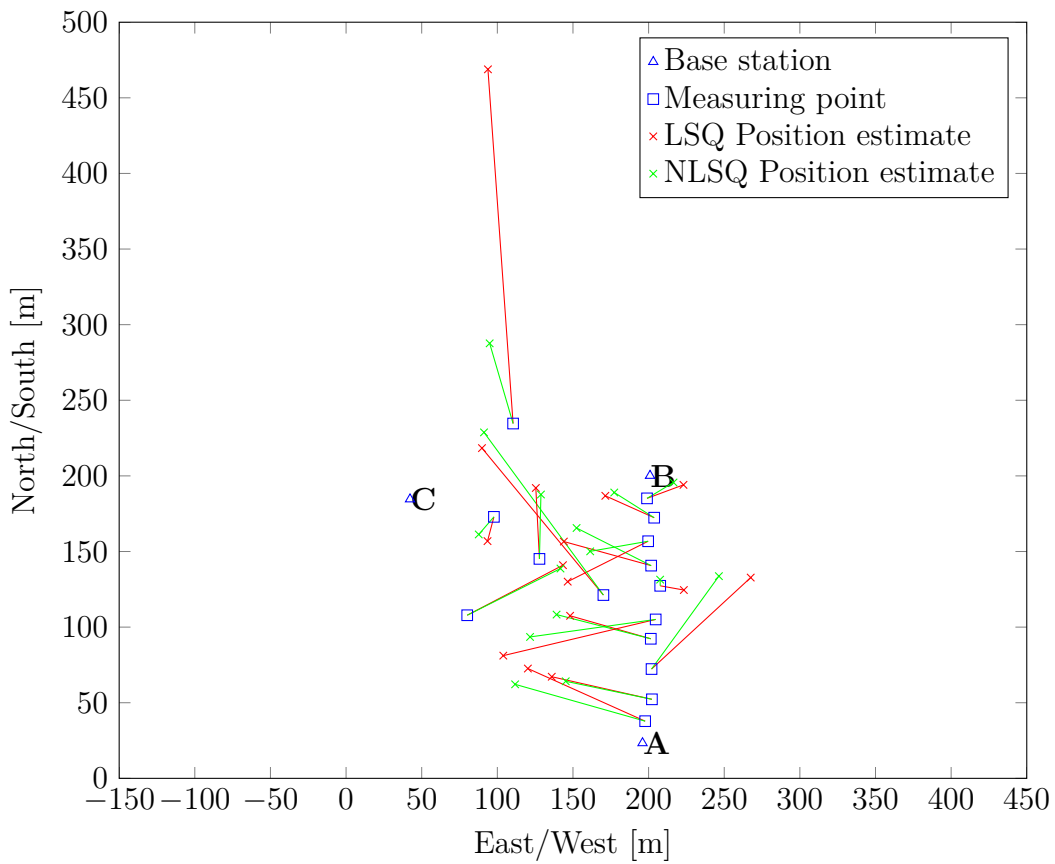
FIGURE 4.10: The estimated positions for both the linear least squares (LSQ) and the non-linear least squares (NLSQ) approximations, plotted along with their corresponding true coordinates.
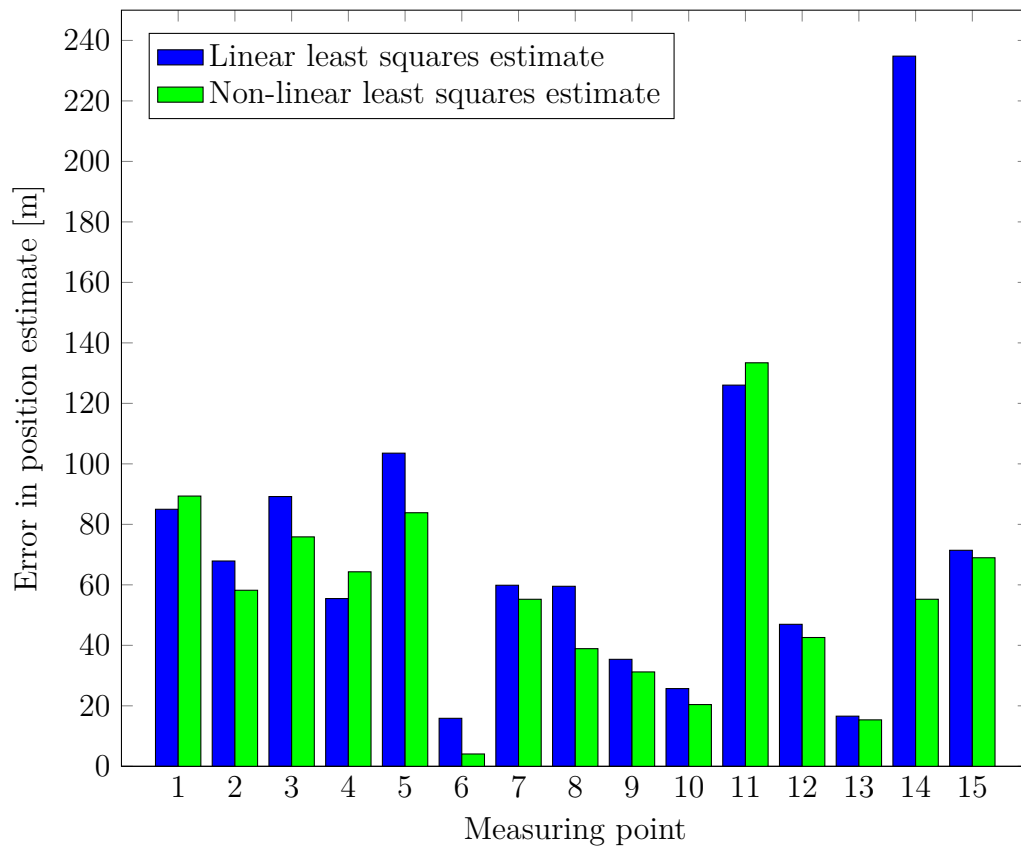
FIGURE 4.11: The position estimate errors in metres for measuring points 1 through 15 for both least squares approximation methods.

Chapter 5

Discussion and conclusion

This chapter will discuss the results from the previous sections further with respect to their significance to the sheep tracking system. A few suggestions for future improvements are given, as well as the final conclusions to this thesis work.

5.1 The method of location

Out of the four different methods of radio location presented in Chapter 2, the two that got selected for further analysis were the

- *Hyperbolic trilateration using TDoA estimates*: This method was preferred because it requires the least amount of communication per location. With this solution, the sheep's transmitter may wake up at a regular interval or according to a predefined schedule, do a clear-channel assessment and transmit a single packet. The packet is picked up by any base stations in range, which would in turn estimate the TDoAs with reference to the GPS-synchronised time standards in each base station. There is no need for the transmitter in the sheep's collar to keep accurate time, and only one transmission is required per location.

- *Circular trilateration based on RSSI measurements*: This method was chosen for its simplicity. Similar to the TDoA method only one transmission from the sheep's radio is required per location. Because this method estimates the absolute range from each base station to the transmitter, there is no need for

accurate time synchronisation between the base stations. However, due to a lot of time-varying factors affecting the signal propagation model, the range estimates are very rough, even under the near-ideal conditions in the RSSI trilateration experiment described in Chapter 4.

The remaining two methods that were not analysed further was:

- *Circular trilateration using ToF estimates*: This requires a query from the base station followed by a reply from the sheep's transmitter to estimate the absolute distance between the two. Since at least three distance estimates are needed, a total of six separate transmissions has to take place per location, compared to the single one required for a TDoA. The accuracy depends on the time taken by the sheep's transmitter to decode the query, and with a fixed and known or negligible delay transmit its reply. The base station needs to measure the time between sending the first packet and receiving the reply. A considerable benefit of using this method is that it does not require the base stations to have a synchronised clock. Yet, because of the six-fold increase in channel use compared to the hyperbolic method and the need for the sheep's transmitter to regularly listen for the queries from the base stations, this method is discarded to save transmission time and energy.

- *Triangulation using direction-of-arrival estimates*: This method was not analysed past the theoretical stage either, firstly because of the added complexity at the base stations; one would need an antenna array as well as a system for accurately detecting phase shifts and subsequently applying a DoA estimation algorithm. Secondly, the expected location error of such a system would, even for highly accurate DoA estimates, grow linearly with the distance between base station and transmitter, an unwanted property in a real-life grazing environment.

5.1.1   Accuracy using TDoA hyperbolic trilateration

As shown in Sections 3.2.1 through 3.2.3, using the CC1120's built-in functionality to determine the time of arrival for a signal did not prove very successful. Of the various signals that were measured, the best results showed an accuracy of about 4 times the symbol rate being used. Under the regulations imposed on location

systems by the Norwegian Post and Telecommunications Authority, the maximum bandwidth for such a system operating in the 169 MHz band is 50 kHz. This limits the symbol rate to 25 ksps, leading to a best-case TDoA accuracy of 10 µs for a pair of base stations. This corresponds to a distance difference of:

$$\Delta_r = 10\,\text{µs} \times 3 \times 10^8\,\text{m s}^{-1} = 3000\,\text{m} \tag{5.1}$$

This uncertainty is too large to enable any form of useful location, which is why the TDoA hyperbolic trilateration based solely on the CC1120 had to be ruled out after this initial testing.

However, the CC1120 has the option to output a bit stream directly from its analog-digital converter (ADC). The ADC process in the CC1120 takes place at the intermediate frequency (IF) stage, at a sampling rate of 16 MHz. Therefore, if the sampled data could be stored directly from the ADC as described in section 3.2.4, the time-delay between two such bit streams from two different base stations should have a time resolution of $\frac{1}{16\,\text{MHz}} = 62.5\,\text{ns}$. Assuming that the bit streams can be time-stamped by clocks in each base station that are synchronized by GPS to within 10 ns as discussed in Section 3.3, the best case accuracy in each TDoA estimate is 72.5 ns, corresponding to a distance resolution of:

$$\Delta_r = 72.5\,\text{ns} \times 3 \times 10^8\,\text{m s}^{-1} = 21.75\,\text{m} \tag{5.2}$$

Unfortunately, developing an FPGA solution set up to decode the 64 MHz LVDS serial bit stream from the CC1120 and store it in buffers, as well as performing cross correlation whenever a signal from the sheep's transmitter is detected, went beyond the scope of this thesis work. A practical test of the TDoA hyperbolic trilateration capabilities of the CC1120 could therefore not be performed, but the solution remains interesting for future work.

Given an error in the TDoA estimate uniformly distributed on $(-72.5\,\text{ns}, 72.5\,\text{ns})$, the error e in the calculated difference of distances will be uniformly distributed and defined by the probability density function $f_E(e) = \frac{1}{21.75-(-21.75)}$, for $e \in (-21.75\,\text{m}, 21.75\,\text{m})$. The mean square error of the difference of distance estimates is given by:

$$\sigma^2 = \int_{-21.75}^{21.75} e^2 f_E(e)\,\text{d}e = \frac{21.75^2}{3} \approx 158 \tag{5.3}$$

The root mean square (RMS) error is then $\sigma = \sqrt{158} \approx 12.6\,\mathrm{m}$ and the resultant RMS error in the position estimates, given the best possible geometry between the base stations and the transmitter is given by equation (2.56):

$$\sqrt{\overline{R_{\min}^2}} = \sqrt{\frac{2\sigma^2}{3}} \approx 10\,\mathrm{m} \tag{5.4}$$

This is a promising result that would be accurate enough to locate sheep on the open range. Although GDoP will affect this accuracy, judging by Figure 2.14 the error will not be greater than twice this number inside the perimeter established by the three base stations.

El Gemayel et al.[23] performed a TDoA trilateration experiment using software-defined radios (USRPs) synchronised by means of GPS receivers. At a sampling rate of $5\,\mathrm{MHz}$ they achieved a root mean square positioning error of about $23\,\mathrm{m}$ for 2000 estimates of a stationary transmitter. Applying a Extended Kalman filter to the position estimates the error was reduced to $10\,\mathrm{m}$. Their TDoA estimates were affected by changing the signal bandwidth and/or the length of the sequences in the cross-correlation. Effects of using other sampling rates are not mentioned.

5.1.2   Accuracy using RSSI circular trilateration

Using the received signal strength as an estimator for the distance between the transmitter and the base station relies heavily on the parameters of the propagation model that is being used. In free space, the signal strength will be inversely proportional to the square of the distance, but in a real-world application many other factors will also apply. For line-of-sight situations, a reasonably reliable estimator for near-ground propagation may be found by taking sample values at known ranges and using e.g. the Theil-Sen approximation to determine the correct path loss exponent as detailed in Section 4.1.2.

Optimizing the propagation model to the actual environment improves the distance estimates. In a real-world system one could use a range of calibration positions throughout the base station network to generate different path loss exponents for the different situations, varying according to for instance:

- *Location*: differences due to if the base station is in dense forest or on an open plain, on a hilltop or a valley floor, and so on.

- *Season*: snow on the ground and on trees would affect the signal propagation, as would foliage that changes with the seasons.

- *Polarization*: the antennas on the base station are fixed, while the ones mounted to the radio collars will be moved about, resulting in a polarization mismatch. Using dipole or monopole antennas, this will influence the received signal strength considerably.

- *Reflection, diffraction and absorption*: depending on the surrounding topography the received signal will include any of these, contributing positively or negatively to the signal strength.

A calibration using values from different known positions throughout the area may also aid a form of "fingerprinting"; a technique frequently used in systems for indoors location where, instead of solving the trilateration problem mathematically, a simple table lookup of the set of RSSI values is performed against a wide set of calibration values (fingerprints). This is especially effective indoors if the required precision is limited to determining the room which the transmitter is in.[24]

5.2 The RSSI trilateration experiment

A location experiment was set up in the Kristiansten park in Trondheim to test the RSSI trilateration method. The base station positions and various measuring points are shown in Figure 4.1, and the estimated distances and positions are presented in Chapter 4.

Most of the distance estimates were accurate to within approximately 60% of the actual range as shown by Figure 5.1. The mean relative error is $\approx 36\%$.

Using these distance estimates, 2-dimensional position estimates were calculated using the Gauss-Newton algorithm, an iterative algorithm for minimization of the squared position error. This resulted in position estimates that were mostly accurate to within about $60\,\mathrm{m}$ as shown in Figure 4.11. The average position of all the position estimates was $55.8\,\mathrm{m}$, and the RMS error was found to be $64.2\,\mathrm{m}$.

As discussed in Section 2.4.1, the distance estimation error is expected to increase proportionally with distance. This means that in the full scale system, where transmitter-base station distances will be up to $5\,\mathrm{km}$, the mean error of 36% in
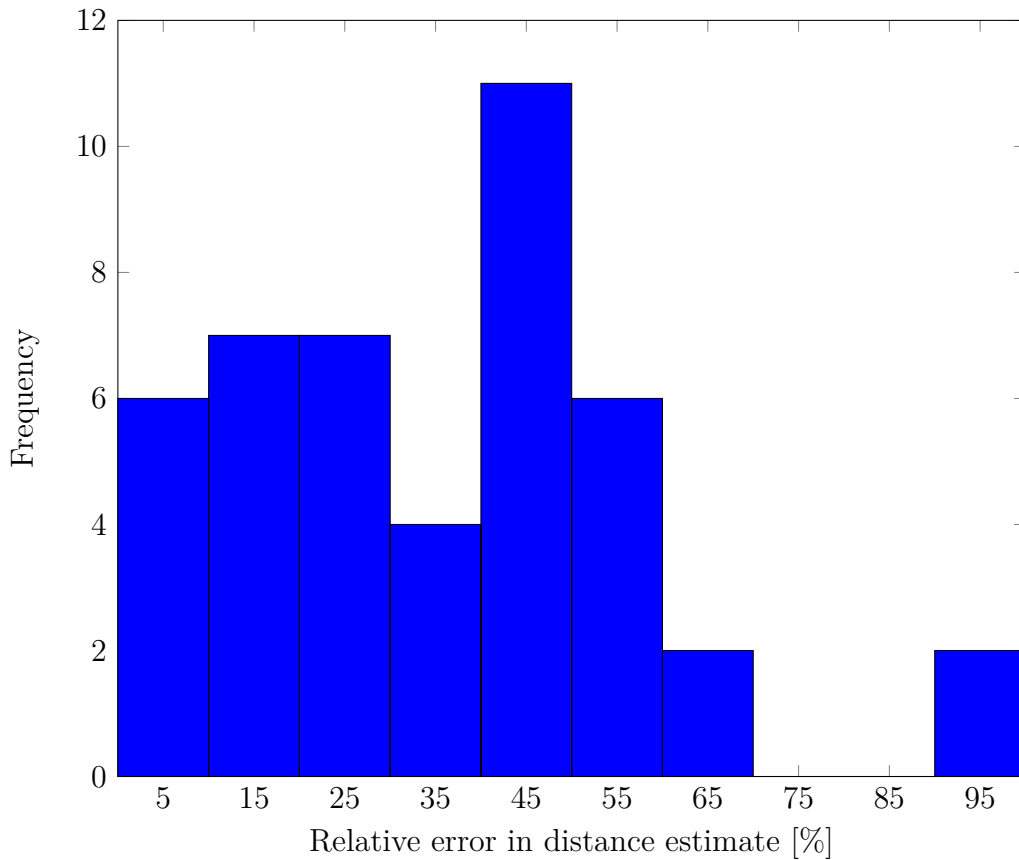
FIGURE 5.1: The distribution of the distance estimation errors relative to the actual range.

the distance estimates means absolute errors of 1.8 km on average. The expected accuracy of the position estimates would then be, at optimal GDoP conditions given by equation (2.43), $\sqrt{2} \times 1.8\,\text{km} \approx 2.55\,\text{km}$. This renders the system unsuitable for locating sheep, especially considering that this estimate is only an up-scaling of the results from the RSSI trilateration experiment, which was performed under near ideal conditions, i.e. most measurements were done having lines of sight to all three base stations and the terrain was open and nearly flat.

The range estimates may be improved to some extent by utilizing diversity schemes such as:

- *Temporal diversity*: In the experiment, 10 packets were sent with an interval of 300 ms. By using more than 10 packets or longer intervals, the final RSSI estimate is based on more data and less vulnerable to time-dependent changes in the propagation environment.

- *Spatial diversity*: Using RSSI measurements taken with the transmitter in slightly modified positions may help to mitigate errors stemming from multi-path effects. In a real-world system, the sheep would be moving, so temporal spacing of the measurements also results in a spatial separation.

- *Frequency diversity*: The RSSI measurements can be taken consecutively using a series of different carrier frequencies. This changes the wavelength between measurements, and helps reduce problems with multi-path interference.

While any of the above-mentioned techniques may improve the 1-dimensional distance estimates, the final estimate for the 2-dimensional position may also be improved by including measurements from more than three base stations, giving the non-linear least squares approximation algorithm more data to work with. In addition it is possible to construct an underlying dynamic model for the sheep's movement. Then, by applying recursive algorithms such as the Kalman filter[25], a more accurate position estimate may be produced based on the previous positions and the dynamic model, as well as the newest data.

That being said, the RSSI measurements are extremely prone to slight variations in the propagation environment, rendering this method of location highly inaccurate when used outdoors and at kilometre-ranges.

5.3 Conclusions and future work

Based on the analysis and experiments in this thesis, the CC1120 proves itself as a easy-to-handle transceiver that performs well in the Sub-GHz band. Its broad selection of integrated features enables the user to test different transmission parameters and modulation schemes without many more peripherals than a micro-controller. For these reasons it is a suitable transceiver choice for both the base stations and the radio collars, especially at an early development stage where the design parameters will change often.

However, the CC1120 cannot facilitate accurate radio location on its own. Experiments using the built-in RSSI functionality to estimate distances proved this method far too inaccurate, with a mean relative error for the distance estimates of 36 %. This resulted in position estimates with an RMS error of 64.2 m with the base stations being set no further apart than about 200 m.

An alternative option is to use the time difference of arrival (TDoA) for pairs of base stations receiving the signal from the radio collar and perform hyperbolic trilateration. Measurements performed on a variety of signals the CC1120 can output that could be used to determine the time of arrival of a signal showed that these are clocked at four times the symbol rate, which gives a best case time resolution of 10 µs for the TDoAs. The resulting uncertainty in position is > 3 km, which is nowhere near the precision needed to locate sheep.

However, a proposed solution using an FPGA to decode the bit stream output of the CC1120's AD-converter directly is expected to yield a time resolution of as little as 62.5 ns. Using GPS receivers at the base stations to provide a synchronised clock, a TDoA accurate to within 72.5 ns could be calculated using cross-correlation between two bit streams from different base stations. Performing the hyperbolic trilateration using TDoA estimates with this accuracy would lead to a position accuracy of approximately 20 m inside the perimeter of the base station network. This is deemed accurate enough to locate sheep on the open range.

Future work should be directed into developing an FPGA-based solution to decode and buffer the bitstream from the CC1120. When this is in place, more accurate TDoA estimates will be available, and the system should be tested on a larger scale to verify the above results.

Appendix A

Numerical results for the RSSI trilateration experiment.

Measuring point	Base station A		Base station B		Base station C	
	True [m]	Est [m]	True [m]	Est [m]	True [m]	Est [m]
1	14.6	13.0	162.4	121.6	213.8	103.0
2	29.6	26.4	147.9	130.7	207.6	133.2
3	49.3	112.8	127.9	67.9	195.2	221.5
4	69.2	38.0	107.9	58.7	184.0	221.5
5	82.2	49.7	95.1	119.3	180.8	71.9
6	104.6	78.7	73.1	37.9	175.0	177.7
7	117.4	128.3	59.5	34.0	165.4	84.5
8	133.5	78.7	43.4	15.3	159.9	78.7
9	149.2	163.0	27.9	16.7	161.9	126.1
10	161.8	171.7	15.1	10.8	156.7	179.9
11	101.2	225.5	84.8	119.3	142.7	70.5
12	139.5	172.2	91.5	44.7	94.2	56.6
13	178.9	159.7	106.7	103.0	56.7	24.1
14	227.9	362.2	96.9	77.2	84.5	75.7
15	143.4	133.2	152.1	89.2	85.5	115.2

TABLE A.1: Numerical data for all the distance estimates from each base station in the RSSI trilateration experiment as well as the true distances.

Measuring point	True position (x, y)	Estimated position (x, y)		Position error [m]	
		LSQ	NLSQ	LSQ	NLSQ
1	197.7, 37.8	120.2, 72.6	111.8, 62.2	85.0	89.4
2	202.2, 52.3	136.0, 67.2	145.2, 64.2	67.9	58.2
3	202.0, 72.3	267.5, 132.8	246.5, 133.7	89.2	75.9
4	201.5, 92.3	148.1, 107.5	139.2, 108.3	55.5	64.3
5	204.7, 105.0	104.0, 81.1	121.6, 93.5	103.5	83.8
6	207.7, 127.3	223.3, 124.5	207.6, 131.4	15.9	4.1
7	201.7, 140.7	144.0, 156.6	152.4, 165.5	59.9	55.2
8	199.7, 156.8	146.5, 130.1	161.4, 150.1	59.5	38.9
9	203.7, 172.4	171.4, 186.8	177.3, 189.0	35.4	31.2
10	199.0, 185.1	223.1, 194.1	216.5, 195.6	25.7	20.4
11	170.1, 121.2	89.8, 218.4	91.2, 228.8	126.0	133.4
12	127.8, 145.1	125.4, 192.0	128.8, 187.7	47.0	42.6
13	97.7, 172.9	93.5, 156.9	87.7, 161.3	16.6	15.4
14	110.4, 234.6	93.8, 468.8	94.9, 287.6	234.8	55.2
15	80.1, 107.9	143.4, 141.0	141.7, 138.7	71.4	69.0

TABLE A.2: The true positions of the measuring points in the RSSI trilateration experiments and the estimated positions and their corresponding error, for both the linear (LSQ) and non-linear least squares (NLSQ) approximations. All coordinates are in the projected (x, y) system.

Appendix B

MATLAB script: Chan's method for hyperbolic trilateration

```matlab
% 15.10.2013 by Snorre H. Olsen
% Linearization of TDoA lateration equations for 3 transmitters.
% Using Chan's method as detailed in "A Simple and Efficient Estimator for
% Hyperbolic Location" by Y. Chan and K. Ho.

%% Initialization %%%%%%%%%%%%%%%%%%%%%%%%%%%%%%%%%%%%%%%%%%%%%%%%%%%%%%%%
clear all; close all;
v0 = 3*10^8;             % Propagation speed of signal
% Base stations (base(:,1)=X-coords, base(:,2)=Y-coords)
base = [-1000,-100;3000,0;1500,2000];
N = length(base);
% Signal source
% The sheep's position as related to the first base station.
source = [3245,1658];    % Unknown in reality

%% Calculation of TDoA values %%%%%%%%%%%%%%%%%%%%%%%%%%%%%%%%%%%%%%%%%%%
% Distances between sheep and each base station
dist = sqrt((source(1)-base(:,1)).^2+(source(2)-base(:,2)).^2);
% Equivalent propagation times:
T = dist./v0;    % Unknown in reality
% Time difference (as referred to the first base station
tau = T-T(1);   % TDoA measurements, measured in reality
% tau = tau+100e-9*randn(1,length(tau));  % Adding timing inaccuracy

%% Trilateration %%%%%%%%%%%%%%%%%%%%%%%%%%%%%%%%%%%%%%%%%%%%%%%%%%%%%%%%
% r: Distance difference r(i) = Ri - R1 according to TDoA measurements.
r = v0.*tau;
% K: Squared distance from base to origin.
K = base(:,1).^2 + base(:,2).^2;
% A: Coefficient matrix for linearised problem Ax=b
A = -1*[base(2,1)-base(1,1), base(2,2)-base(1,2);...
        base(3,1)-base(1,1), base(3,2)-base(1,2)];
Ai = inv(A);
% Solution of eq.set in terms of R1, x = S*R1+T,y = U*R1+V
```

```matlab
S = Ai(1,1)*r(2) + Ai(1,2)*r(3);
T = 0.5*( Ai(1,1)*(r(2)^2-K(2)+K(1)) + Ai(1,2)*(r(3)^2-K(3)+K(1)) );

U = Ai(2,1)*r(2)+Ai(2,2)*r(3);
V = 0.5*( Ai(2,1)*(r(2)^2-K(2)+K(1)) + Ai(2,2)*(r(3)^2-K(3)+K(1)) );
% Quadratic equation in R1: a*R1^2+b*R1+c = 0  as a result of inserting
% above solution into expanded equation for R1^2.
a = 1-S^2-U^2;
b = 2*(base(1,1)*S + base(1,2)*U - S*T - U*V);
c = 2*base(1,1)*T + 2*base(1,2)*V - T^2 - V^2 - K(1);
% Solving for R1 using the quadratic formula.
% R1: Distance from transmitter to receiver 1.
R1pos = (-1*b+sqrt(b^2-4*a*c))/(2*a);
R1neg = (-1*b-sqrt(b^2-4*a*c))/(2*a);

% Select positive solution. If both posistive set R1 = 0. (ambiguity error)
R1 = (R1pos*(R1pos>0)+R1neg*(R1neg>0))*((R1pos<0)||(R1neg<0))
% Insert solution for R1 back into equations for x and y;
x = S*R1 + T        % Calculated x coordinate
y = U*R1 + V        % Calculated y coordinate
```

Appendix C

MATLAB script: The Gauss-Newton minimization algorithm

```matlab
function [ pos, history ] = newtonPos2D( bs, rEst, init, steps, thr)
%NEWTONPOS2D Uses Newton's iterative method to approximate a solution to
%               the trilateration problem in 2 dimensions.
%   Input:
%     bs:    Base station positions. One row [x y] for each base station.
%      r:    Range estimates, one row for each base station.
%   init:    Initial position estimate [x y]
%  steps:    Max no. of iteration steps
%    thr:    Threshold for stopping the iteration
%   Output:
%     R:     Estimated position [x y]
%
% Given a set of base station coordinates, range estimates to the unknown
% transmitter and a initial position estimate, this iterative algorithm
% will work to find a non-linear least squares approximation until either
% the maximum number of steps or the minimum step length  for each
% iteration is reached.
% By Snorre H. Olsen, 20.05.2014

pos = init;      % Initial guess for position.
del = thr;       % Dummy step length to start iteration
k=1;             % Iteration counter
while(del>=thr && k<=steps)
    r = sqrt((pos(1)-bs(:,1)).^2+(pos(2)-bs(:,2)).^2);
    % JtJ is transpose of J times J where J is the Jacobian for the
    % function f_i = r_i - rEst_i:
    JtJ = [...
        sum((pos(1)-bs(:,1)).^2./r.^2), sum((pos(1)-bs(:,1)).*(pos(2)-bs(:,2))./r.^2) ;...
        sum((pos(1)-bs(:,1)).*(pos(2)-bs(:,2))./r.^2), sum((pos(2)-bs(:,2)).^2./r.^2)];
    % Jtf is the transpose of J times f where f is a column vector
    % containing f_i = r_i - rEst_i for this iteration step:
```

```matlab
    Jtf = [...
        sum((r-rEst).*(pos(1)-bs(:,1))./r);...
        sum((r-rEst).*(pos(2)-bs(:,2))./r)];
    % Iteration: the next estimate is calculated:
    posNext = pos - (JtJ\Jtf)';

    del = sqrt(sum((pos-posNext).^2));   % Step length in this iteration.
    history(k,:) = posNext;              % Logging iterations for plotting.

    pos = posNext;
    k=k+1;
end

end
```

Appendix D

Key Characteristics of the CC1120

High Performance RF Transceiver for Narrowband Systems

Applications

Narrowband ultra low power wireless systems with channel spacing down to 12.5 kHz

170/315/433/868/915/920/950 MHz ISM/SRD band

Wireless Metering and Wireless Smart Grid (AMR and AMI)

IEEE 802.15.4g systems

Home and building automation

Wireless alarm and security systems

Industrial monitoring and control

Wireless healthcare applications

Wireless sensor networks and Active RFID

Private mobile radio

Regulations

Suitable for systems targeting compliance with:

Europe	ETSI EN 300 220
	ETSI EN 54-25
US	FCC CFR47 Part 15
	FCC CFR47 Part 90, 24 and 101
Japan	ARIB RCR STD-T30
	ARIB STD-T67
	ARIB STD-T108

Key Features

High performance single chip transceiver

- o Adjacent channel selectivity: 64 dB at 12.5 kHz offset
- o Blocking performance: 91 dB at 10 MHz offset
- o Excellent receiver sensitivity:
  - -123 dBm at 1.2 kbps
  - -110 dBm at 50 kbps
  - -127 dBm using built-in coding gain
- o Very low phase noise: -111 dBc/Hz at 10 kHz offset

Suitable for systems targeting ETSI category 1 compliance in 169 MHz and 433 MHz bands

High spectral efficiency (9.6 kbps in 12.5 kHz channel in compliance with FCC narrowbanding mandate)

Power Supply
- o Wide supply voltage range (2.0 V – 3.6 V)
- o Low current consumption:
  - RX: 2 mA in RX Sniff Mode
  - RX: 17 mA peak current in low power mode
  - RX: 22 mA peak current in high performance mode
  - TX: 45 mA at +14 dBm
- o Power down: 0.3 µA

Programmable output power up to +16 dBm with 0.4 dB step size

Automatic output power ramping

Configurable data rates: 0 to 200 kbps

Supported modulation formats: 2-FSK, 2- GFSK, 4-FSK, 4-GFSK, MSK, OOK

WaveMatch: Advanced digital signal processing for improved sync detect performance

RoHS compliant 5x5mm QFN 32 package

Peripherals and Support Functions

Enhanced Wake-On-Radio functionality for automatic low-power receive polling

Separate 128-byte RX and TX FIFOs

Includes functions for antenna diversity support

Support for re-transmissions

Support for auto-acknowledge of received packets
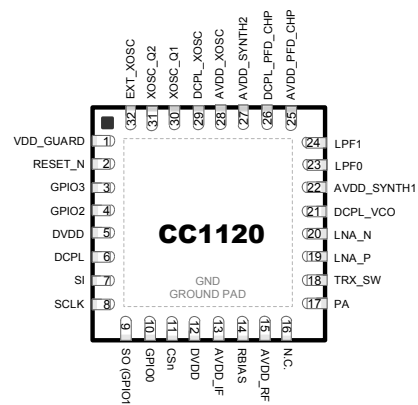
TCXO support and control, also in power modes

Automatic Clear Channel Assessment (CCA) for listen-before-talk (LBT) systems

Built in coding gain support for increased range and robustness

Digital RSSI measurement

Support for seamless integration with the **CC1190** for increased range giving up to 3 dB improvement in sensitivity and up to +27 dBm output power

Temperature sensor

Description

The **CC1120** is a fully integrated single-chip radio transceiver designed for high performance at very low power and low voltage operation in cost effective wireless systems. All filters are integrated, removing the need for costly external SAW and IF filters. The device is mainly intended for the ISM (Industrial, Scientific and Medical) and SRD (Short Range Device) frequency bands at 164-192 MHz, 274-320 MHz, 410-480 MHz and 820-960 MHz.

The **CC1120** provides extensive hardware support for packet handling, data buffering, burst transmissions, clear channel assessment, link quality indication and Wake-On-Radio. The **CC1120** main operating parameters can be controlled via an SPI interface. In a typical system, the **CC1120** will be used together with a microcontroller and only few external passive components.

Bibliography

[1] Statens Landbruksforvaltning. Nasjonalt beiteprosjekt 2009-2012, sluttrapport. Final report, Statens Landbruksforvaltning, 2013.

[2] A. S. Haugset and G. Nossum. Elektronisk overvåkning av sau på utmarksbeite i nord-trøndelag. Final report., Trøndelag Forskning og Utvikling AS, 2010.

[3] W Murphy and Willy Hereman. Determination of a position in three dimensions using trilateration and approximate distances. *Department of Mathematical and Computer Sciences, Colorado School of Mines, Golden, Colorado, MCS-95-07*, 19, 1995.

[4] Charles L Lawson and Richard J Hanson. *Solving least squares problems*. Society for Industrial and Applied Mathematics, 1974.

[5] R Penrose. A generalized inverse for matrices. In *Proceedings of the Cambridge Philosophical Society*, volume 51, pages 406–413, 1955.

[6] Ake Björck. *Numerical methods for least squares problems*. Society for Industrial and Applied Mathematics, 1996.

[7] W. Hahn and S. Tretter. Optimum processing for delay-vector estimation in passive signal arrays. *Information Theory, IEEE Transactions on*, 19(5):608–614, Sep 1973.

[8] W.H. Foy. Position-location solutions by Taylor-series estimation. *Aerospace and Electronic Systems, IEEE Transactions on*, AES-12(2):187–194, March 1976.

[9] JS Abel and J Smith. The spherical interpolation method for closed-form passive source localization using range difference measurements. In *Acoustics, Speech, and Signal Processing, IEEE International Conference on ICASSP'87.*, volume 12, pages 471–474. IEEE, 1987.

[10] Y. T. Chan and K. C. Ho. A simple and efficient estimator for hyperbolic location. *IEEE Transactions on Signal Processing*, 42(8):1905–1915, August 1994.

[11] B.T. Fang. Simple solutions for hyperbolic and related position fixes. *Aerospace and Electronic Systems, IEEE Transactions on*, 26(5):748–753, Sep 1990.

[12] Constantine A Balanis. *Antenna theory: analysis and design.* John Wiley & Sons, 3 edition, 2012.

[13] *CC112X/CC1175 Low-Power High Performance Sub-1GHz RF Transceiver/- Transmitter User's Guide.* Texas Instruments, 2013.

[14] Steven Lanzisera, David Zats, and Kristofer S. J. Pister. Radio frequency time-of-flight distance measurement for low-cost wireless sensor localization. *IEEE Sensors Journal*, 11(3):837–845, March 2011.

[15] David Tse and Pramod Viswanath. *Fundamentals of Wireless Communication.* Cambridge University Press, 2005.

[16] Børje Forssell. *Radionavigation Systems.* Prentice Hall International, UK, 1991.

[17] D.L. Mills. Internet time synchronization: the network time protocol. *Communications, IEEE Transactions on*, 39(10):1482–1493, Oct 1991.

[18] *TrxEB RF PER Test Software Example User Guide.* Texas Instruments, swru296b edition, 2013.

[19] K. Aamodt. Application note AN042, the CC2431 location engine. Technical Report SWRA095, Texas Instruments, 2006.

[20] Katayoun Sohrabi, Bertha Manriquez, and Gregory J. Pottie. Near ground wideband channel measurement in 800-1000 mhz. In *1999 IEEE 49th Vehicular Technology Conference*, pages 571–574. The Institute of Electrical and Electronics Engineers, Inc., 1999.

[21] Ronald E. Walpole, Raymond H. Myers, Sharon L. Myers, and Keying E. Ye. *Probability and Statistics for Engineers and Scientists.* Pearson Higher Education, 9 edition, 2012.

[22] Henri Theil. A rank-invariant method of linear and polynomial regression analysis. *Nederl. Akad. Wetensch., Proc.*, 53:386–392, 1950.

[23] Noha El Gemayel, Sebastian Koslowski, Friedrich K Jondral, and Joachim Tschan. A low cost tdo localization system: Setup, challenges and results. In *Positioning Navigation and Communication (WPNC), 2013 10th Workshop on*, pages 1–4. IEEE, 2013.

[24] Ville Honkavirta, Tommi Perala, Simo Ali-Loytty, and Robert Piché. A comparative survey of wlan location fingerprinting methods. In *6th Workshop on Positioning, Navigation and Communication, 2009.*, pages 243–251. IEEE, 2009.

[25] Rudolph Emil Kalman. A new approach to linear filtering and prediction problems. *Journal of Fluids Engineering*, 82(1):35–45, 1960.